Source apportionment of ultrafine particles in urban Europe

Meritxell Garcia-Marlès, Rosa Lara, Cristina Reche, Noemí Pérez, Aurelio Tobías, Marjan Savadkoohi, David Beddows, Imre Salma, Máté Vörösmarty, Tamás Weidinger, et al.

Environment International 194 (2024) 109149

Contents lists available at ScienceDirect

Environment International

journal homepage: www.elsevier.com/locate/envint

Full length article

Source apportionment of ultrafine particles in urban Europe

Meritxell Garcia-Marlès [a,b,*], Rosa Lara [a], Cristina Reche [a], Noemí Pérez [a], Aurelio Tobías [a], Marjan Savadkoohi [a,c], David Beddows [d], Imre Salma [e], Máté Vörösmarty [f], Tamás Weidinger [g], Christoph Hueglin [h], Nikos Mihalopoulos [i,j], Georgios Grivas [j], Panayiotis Kalkavouras [j,k], Jakub Ondracek [l], Nadezda Zikova [l], Jarkko V. Niemi [m], Hanna E. Manninen [m], David C. Green [n,o], Anja H. Tremper [n], Michael Norman [p], Stergios Vratolis [q], Evangelia Diapouli [q], Konstantinos Eleftheriadis [q], Francisco J. Gómez-Moreno [r], Elisabeth Alonso-Blanco [r], Alfred Wiedensohler [s], Kay Weinhold [s], Maik Merkel [s], Susanne Bastian [t], Barbara Hoffmann [u], Hicran Altug [u], Jean-Eudes Petit [v], Prodip Acharja [v], Olivier Favez [w], Sebastiao Martins Dos Santos [x], Jean-Philippe Putaud [x], Adelaide Dinoi [y], Daniele Contini [y], Andrea Casans [z], Juan Andrés Casquero-Vera [z], Suzanne Crumeyrolle [aa], Eric Bourrianne [aa], Martine Van Poppel [ab], Freja E. Dreesen [ac], Sami Harni [ad], Hilkka Timonen [ad], Janne Lampilahti [ae], Tuukka Petäjä [ae], Marco Pandolfi [a], Philip K. Hopke [af], Roy M. Harrison [d,ag], Andrés Alastuey [a], Xavier Querol [a,*]

[a] Institute of Environmental Assessment and Water Research (IDAEA-CSIC), 08034 Barcelona, Spain
[b] Department of Applied Physics-Meteorology, University of Barcelona, Barcelona, 08028, Spain
[c] Department of Mining, Industrial and ICT Engineering (EMIT), Manresa School of Engineering (EPSEM), Universitat Politècnica de Catalunya (UPC), Manresa, 08242, Spain
[d] Division of Environmental Health and Risk Management, School of Geography, Earth and Environmental Sciences University of Birmingham, Edgbaston, Birmingham, B15 2TT, United Kingdom
[e] Institute of Chemistry, Eötvös Loránd University, Budapest, Hungary
[f] Hevesy György Ph.D. School of Chemistry, Eötvös Loránd University, Budapest, Hungary
[g] Department of Meteorology, Institute of Geography and Earth Sciences, Eötvös Loránd University, Budapest, Hungary
[h] Laboratory for Air Pollution and Environmental Technology, Swiss Federal Laboratories for Materials Science and Technology (Empa), 8600 Duebendorf, Switzerland
[i] Environmental Chemical Processes Laboratory, Department of Chemistry, University of Crete, 71003 Heraklion, Greece
[j] Institute for Environmental Research & Sustainable Development, National Observatory of Athens, 11810 Athens, Greece
[k] Department of Environment, University of the Aegean, 81100 Mytilene, Greece
[l] Research Group of Aerosol Chemistry and Physics, Institute of Chemical Process Fundamentals, v.v.i., Academy of Sciences of the Czech Republic, Rozvojova 1, Prague, Czech Republic
[m] Helsinki Region Environmental Services Authority (HSY), 00240 Helsinki, Finland
[n] MRC Centre for Environment and Health, Environmental Research Group, Imperial College London, United Kingdom
[o] NIHR HPRU in Environmental Exposures and Health, Imperial College London, United Kingdom
[p] Environment and Health Administration, SLB-analys, Box 8136, 104 20 Stockholm, Sweden
[q] ENRACT, Institute of Nuclear and Radiological Science & Technology, Energy & Safety, NCSR Demokritos, 15310 Ag. Paraskevi, Athens, Greece
[r] Department of Environment, CIEMAT, Madrid, 28040, Spain
[s] Leibniz Institute for Tropospheric Research (TROPOS), Leipzig, Germany
[t] Saxon State Office for Environment, Agriculture and Geology (LfULG), Dresden, German
[u] Institute for Occupational, Social and Environmental Medicine, Medical Faculty and University Hospital Düsseldorf, Heinrich Heine University Düsseldorf, Germany
[v] Laboratoire des Sciences du Climat et de l'Environnement, CEA/Orme des Merisiers, 91191 Gif-sur-Yvette, France
[w] Institut National de l'Environnement Industriel et des Risques (INERIS), Parc Technologique Alata BP2, 60550 Verneuil-en-Halatte, France
[x] European Commission, Joint Research Centre (JRC), 21027 Ispra, Italy
[y] Institute of Atmospheric Sciences and Climate of National Research Council, ISAC-CNR, 73100 Lecce, Italy
[z] Andalusian Institute for Earth System Research (IISTA-CEAMA), University of Granada, Granada, Spain
[aa] University Lille, CNRS, UMR 8518 Laboratoire d'Optique Atmosphérique (LOA), Lille, France

* Corresponding authors.
E-mail addresses: meri.garcia@idaea.csic.es (M. Garcia-Marlès), xavier.querol@idaea.csic.es (X. Querol).

https://doi.org/10.1016/j.envint.2024.109149
Received 5 July 2024; Received in revised form 16 October 2024; Accepted 11 November 2024
Available online 15 November 2024

[ab] Flemish Institute for Technological Research (VITO), Boeretang 200, 2400 Mol, Belgium
[ac] Flanders Environment Agency, Dokter De Moorstraat 24-26, 9300, Aalst, Belgium
[ad] Finnish Meteorological Institute, Atmospheric Composition Research, Helsinki, Finland
[ae] Institute for Atmospheric and Earth System Research (INAR), Faculty of Science, University of Helsinki, Finland
[af] Department of Public Health Sciences, University of Rochester School of Medicine & Dentistry, Rochester, NY 14642, USA
[ag] Department of Environmental Sciences, Faculty of Meteorology, Environment and Arid Land Agriculture, King Abdulaziz University, Jeddah, Saudi Arabia

ARTICLE INFO

Keywords:
Positive matrix factorization
Ultrafine particles
Particle number size distributions
Air quality
Traffic emissions
New particle formation

ABSTRACT

There is a body of evidence that ultrafine particles (UFP, those with diameters $\leq$ 100 nm) might have significant impacts on health. Accordingly, identifying sources of UFP is essential to develop abatement policies. This study focuses on urban Europe, and aims at identifying sources and quantifying their contributions to particle number size distribution (PNSD) using receptor modelling (Positive Matrix Factorization, PMF), and evaluating long-term trends of these source contributions using the non-parametric Theil-Sen's method. Datasets evaluated include 14 urban background (UB), 5 traffic (TR), 4 suburban background (SUB), and 1 regional background (RB) sites, covering 18 European and 1 USA cities, over the period, when available, from 2009 to 2019. Ten factors were identified (4 road traffic factors, photonucleation, urban background, domestic heating, 2 regional factors and long-distance transport), with road traffic being the primary contributor at all UB and TR sites (56–95 %), and photonucleation being also significant in many cities. The trends analyses showed a notable decrease in traffic-related UFP ambient concentrations, with statistically significant decreasing trends for the total traffic-related factors of −5.40 and −2.15 % yr^{-1} for the TR and UB sites, respectively. This abatement is most probably due to the implementation of European emissions standards, particularly after the introduction of diesel particle filters (DPFs) in 2011. However, DPFs do not retain nucleated particles generated during the dilution of diesel exhaust semi-volatile organic compounds (SVOCs). Trends in photonucleation were more diverse, influenced by a reduction in the condensation sink potential facilitating new particle formation (NPF) or by a decrease in the emissions of UFP precursors. The decrease of primary PM emissions and precursors of UFP also contributed to the reduction of urban and regional background sources.

1. Introduction

Particulate matter (PM) is recognized as a major air pollutant due to its well-established harmful effects on human health. Evidence points to its association with respiratory and cardiovascular diseases, among others, as well as increased mortality (WHO, 2021a). These health impacts are influenced both by the size and composition of the particles. Ultrafine particles, defined as particles with diameters less than 100 nm, contribute a very small fraction to the PM mass concentrations (measured in terms of mass per unit volume, μg m^{-3}) but represent a substantial portion of particle number concentrations (PNC, measured in particles per cubic centimetre, # cm^{-3}). In urban environments, UFPs contribute to 84 ± 3.7 % of total PNC, based on data from 27 studies across Europe (Trechera et al., 2023). Consequently, PNC is frequently utilized as a surrogate for UFP. Particle number size distributions (PNSD) are measured by calculating PNCs for specific size ranges. PNSDs categorize particle into three size modes: Nucleation (<25 nm), Aitken (25–100 nm) and Accumulation (100–1000 nm) (Seinfeld and Pandis, 2016; CEN, 2020; ISO, 2023). It is important to highlight that ambient UFP concentrations are not regulated by the EU's ambient air quality standards, while PM is (2008/50/CE, EC, 2008). However, the draft for a new proposal of an EU air quality directive (EC, 2023) requires both UFP and PNSD measurements to be implemented in routine air quality monitoring supersites, together with black carbon (BC), ammonia (NH_3), and other advanced air quality parameters.

Despite the increasing attention on UFPs, the epidemiological results regarding their health effects are often inconsistent (Ohlwein et al., 2019; US EPA, 2019; WHO, 2021b). Cassee et al. (2019) and Rivas et al. (2021) reported that inconsistency in short-term health effects studies might be due to the lack of standardization in UFP measurement methods, limited long-term data available for analysis, the high variability of UFP concentrations in both space and time, the limited representation of human exposure to UFPs resulting from the use of only one monitoring station per city in most studies, and the different sources contributing to UFP concentrations in each region. While the most recent WHO Air Quality Guidelines did not establish specific guidelines for UFP or PNC, they recommend more extensive, harmonised measurements to assess whether establishing specific guidelines is warranted (WHO, 2021b). CEN (2020), ACTRIS (2021), RI-URBANS (2022) and Trechera et al. (2023) have suggested that total PNC should be measured with a lower size detection limit of 10 nm, and PNSDs should be assessed over a range of 10 to 800 nm.

Identifying the UFP sources and their contributions is essential to develop cost-effective abatement policies, since several studies suggest that negative health effects may be enhanced with decreasing particle size. Thus, the small size of UFPs allows them to penetrate deep into the respiratory system, potentially translocating through the alveoli and affecting various organs (Oberdörster et al., 2005; Peters et al., 2006; Kreyling et al., 2014; Salma et al., 2015; Cassee et al., 2019). This behaviour has been linked to an increased risk of premature mortality (Wichmann et al., 2000; Ibald-Mulli et al., 2004; Tobías et al., 2018; Schwarz et al., 2023).

Typically, receptor models for source apportionment use chemical composition data to provide information on sources of PM mass concentrations (Amato and Hopke, 2012; Pancras et al., 2013; Amato et al., 2016; Zíková et al., 2016; Taghvaee et al., 2018). However, sources dominating PNC differ from those dominating particle PM mass concentrations, thus a number of studies applied receptor modelling for the source apportionment of UFP-PNSD, using the variability of the PNSD instead of the chemical composition (Liu et al., 2014; Brines et al., 2014; Beddows et al., 2015; Sowlat et al., 2016; Rivas et al., 2019; Vörösmarty et al., 2024; Xu et al., 2024). Hopke et al. (2022) identified 55 peer-review articles reporting source apportionment of PNSD in 102 locations/time periods. Almost all of these studies were performed with Positive Matrix Factorization (PMF, Paatero and Tapper, 1994), the most frequently used receptor modelling method (Ogulei et al., 2007; Liu et al., 2014; Beddows et al., 2015; Rivas et al., 2019; Squizzato et al., 2019; Hopke et al., 2023). However, other methodologies were also used such as Principal Component Analysis (PCA, Wehner and Wiedensohler, 2003; Chan and Mozurkewich, 2007; Oliveira et al., 2009; Pey et al., 2009; Cusack et al., 2013; Khan et al., 2015) and k-means clustering (Beddows et al., 2009; Dall'Osto et al., 2012, 2019; Wegner et al., 2012; Brines et al., 2014, 2015; Chen et al., 2021). Rodríguez and Cuevas (2007) also developed a methodology to split PNCs affected by fresh

vehicle exhaust emissions into two components: N1, accounting for primary particles directly emitted in the particle phase or nucleating immediately after the emissions, and N2, accounting for the new particle formation (NPF) and other secondary UFP. Casquero-Vera et al. (2021) refined this method to estimate N1 from traffic and biomass burning sources.

Studies on source apportionment of UFPs in urban areas identify road traffic as the main source (Zhou et al., 2005; Pey et al., 2009; Dall'Osto et al., 2012; Harrison et al., 2011; Kumar et al., 2014; Brines et al., 2015; Beddows and Harrison, 2019; Rivas et al., 2019; Hopke et al., 2022, 2024; Kalkavouras et al., 2024), typically accounting for > 70 % of the annual UFP emissions (Hopke et al., 2022). Particles emitted from vehicles can be formed in the engine or in the atmosphere after emission from the tailpipe (Charron and Harrison, 2003; Kumar et al., 2014; Rönkkö and Timonen, 2019; Damayanti et al., 2023). Two traffic sources are usually reported with two major number modes with peaks around 30–35 nm, commonly ascribed to spark-ignition (gasoline) vehicles, and 60–80 nm, associated with diesel vehicle emissions (Ogulei et al., 2007; Liu et al., 2014; Hopke et al., 2022; Vörösmarty et al., 2024). It is also suggested that the smaller mode particles represent freshly traffic particles emitted by vehicles on nearby roads (Gu et al., 2011), or that can be associated to nucleation of particles generated during dilution of diesel exhaust semi-volatile organic compounds (SVOCs) (Harrison et al., 2011; Damayanti et al., 2023). The larger mode is also associated with the coagulation of the particles moving away from the sources, i.e., aged traffic emission (Zhu et al., 2002; Gu et al., 2011). However, traffic exhaust emissions also result in particles smaller than 30 nm in diameter, both as primary emissions (Rönkkö et al., 2017) and due to the nucleation of the particles immediately after the emission to the atmosphere as they dilute and cool, leading to delayed primary particles (Harrison et al., 2011; Trechera et al., 2023).

Besides traffic, other sources contribute to UFP. Photochemical nucleation lead to NPF events, characterised by PNSD peaking at the finest sizes. These events are enhanced by high insolation and wind speed, low relative humidity, low pre-existing particle surface area (i.e., low condensation sink) and available precursor gases such as SO_2 (Kulmala and Kerminen, 2008; Brines et al., 2015; Trechera et al., 2023). Emissions from harbours and airports also typically prevail in the Nucleation mode (Westerdahl et al., 2008; Keuken et al., 2015; Rivas et al., 2019; Stacey et al., 2020). Other sources identified contributing to urban UFP concentrations are characterised by modes close to or coarser than 100 nm, such as urban background (with high load from traffic), domestic heating, regional background and long-range transport.

There are only a few available studies analysing long-term trends of UFP (Simon et al., 2020; Mikkonen et al., 2020; Presto et al., 2021; Chen et al., 2022; Damayanti et al., 2023; Garcia-Marlès et al., 2024). Garcia-Marlès et al. (2024) evaluated 2009–2019 trends of UFP concentrations and different particle size modes, based on PNSD measurements from 21 sites from 15 European and 1 USA cities. The results showed significant decreases in the Aitken and Accumulation modes, suggesting a positive impact of the implementation of EURO 5/V and 6/VI vehicle standards on European air quality and the growing use of Diesel Particle Filters (DPF), but inconsistent results in the Nucleation mode particles due to insufficient controls. Additionally, long-term trends in the contribution of UFP sources can also be analysed. However, most of the studies on source apportionment of UFP did not cover periods long enough to perform trend analyses of source-specific PNCs. Recently, Hopke et al. (2024) conducted the source apportionment of PNSD from a site in USA (Rochester, New York) covering a long period and analysed the trends of the sources.

The project RI-URBANS (Research Infrastructures Services Reinforcing Air Quality Monitoring Capacities in European Urban & Industrial Areas) is a European research initiative funded by the European Union's Horizon 2020 program (grant 101036245). Its primary goal is to develop tools for the measurement and analysis of advanced air quality parameters, with the aim of enhancing pollution control, improving air quality policies, and assessing health impacts. A key focus of RI-URBANS is the measurement and application of UFP-PNSD in air quality assessments. Prior RI-URBANS studies analysed UFP in urban Europe. Trechera et al. (2023) reported the phenomenology of UFP and compared 2017–2019 concentrations across different cities and environments, Liu et al. (2023) calculated and evaluated aerosol Lung Deposited Surface Area (LDSA) concentrations, and Garcia-Marlès et al. (2024) focused on the long-term trends of UFP. In line with these, the present study aims to identify and quantify sources contributing to UFP-PNSD using the receptor model PMF, and to assess long-term trends of the source contributions. The source apportionment of 24 datasets is conducted for a period covering up to 11 years (2009–2019), when available.

2. Methodology

2.1. Monitoring sites and instrumentation

This study analyses 24 PNSD datasets collected between 2009 and 2019, with data coverage ranging from 3 to 11 years. These data were compiled by the RI-URBANS project and supplied from advanced air quality monitoring networks and research sites, and already used with other purposes in previous studies by Trechera et al. (2023), Liu et al. (2023) and Garcia-Marlès et al. (2024). The data covers 24 sites across 18 European cities and one in the USA, with different climate and urban structure patterns, UFP concentrations and sources. These sites include (see Fig. 1 and Table 1):

- Fourteen urban background (UB) sites: Antwerp (ANT_UB), Athens (ATH_UB), Barcelona (BCN_UB), Budapest (BUD_UB), Dresden (DRE_UB), Granada (GRA_UB), Helsinki (HEL_UB), Lecce (LEC_UB), Leipzig (LEI_UB), London (LND_UB), Madrid (MAD_UB), Mülheim (MUL_UB), Zurich (ZUR_UB), and Rochester (ROC_UB) in New York State in USA.
- Five traffic (TR) sites: Dresden (DRE_TR), Helsinki (HEL_TR), Leipzig (LEI_TR), London (LND_TR) and Stockholm (STO_TR).
- Four suburban background (SUB) sites: Athens (ATH_SUB), Lille (LIL_SUB), Paris (PAR_SUB) and Prague (PRA_SUB).
- One regional background (RB) site: Ispra (IPR_RB).

Hourly PNSD averages were used in this study, with data restricted to 2019 to avoid the influence of pollution reductions caused by COVID19-lockdowns, as noted in several studies (Salma et al., 2020; Dinoi et al., 2021; Eleftheriadis et al., 2021; Petit et al., 2021; Putaud et al., 2021, 2023).

In addition to the PNSD data, ancillary pollutants (including BC, NO_2, NO, CO, SO_2, O_3, PM_{10}, $PM_{2.5}$ and PM_1) were collected where available (see Table 1). These measurements were taken either from the same monitoring locations or nearby air quality monitoring sites, by instrumentation fulfilling European standards. PNSD data used in this analysis is publicly accessible through the EBAS database (https://ebas.nilu.no/).

PNSD datasets were collected using different types and models of Mobility Particle Size Spectrometer (MPSS), as detailed in Table S1. Although ACTRIS (2021) and CEN (2020) guidelines recommend a measurement size range of 10–800 nm, some instruments had coarser lower detection limits, starting above the recommended 10 nm. Furthermore, drastic concentration jumps were detected in the lower sizes in some datasets, thus these ranges were removed. Consequently, 50 % of the sites (BCN_UB, BUD_UB, GRA_UB, LND_UB, MAD_UB, MUL_UB, ROC_UB, ZUR_UB, HEL_TR, LND_TR, LIL_SUB, PAR_SUB) started measurement between 11 and 20 nm. As stated by Trechera et al. (2023), the lower size detection significantly affects the total PNC, thus this variation must be accounted for when comparing sources with PNC prevalence in the Nucleation mode.

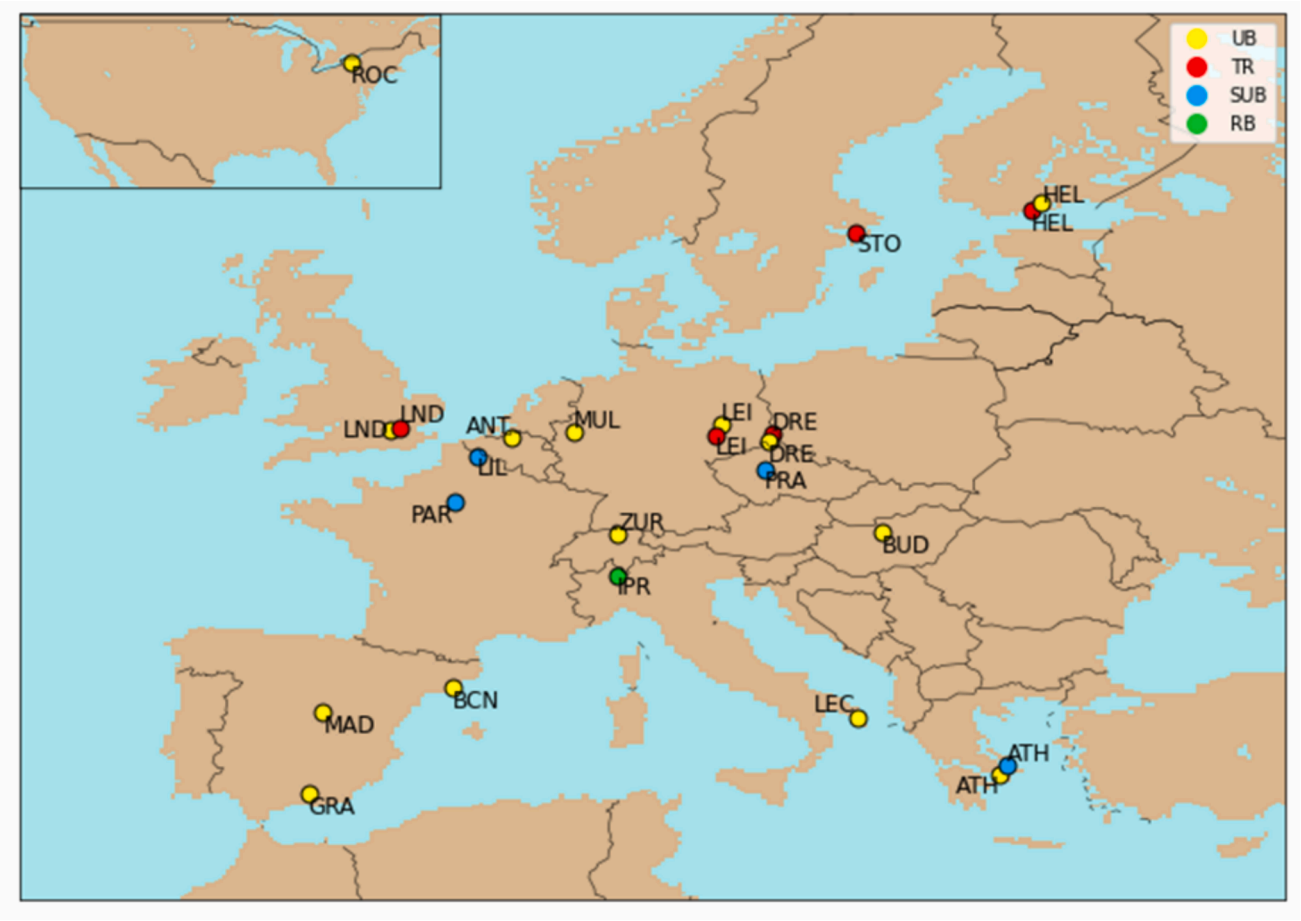

Fig. 1. Map showing the location of the cities and type of stations providing data on particle number concentration (PNC) and particle number size distribution (PNSD). Station categories include Urban background (UB), Traffic (TR), Suburban background (SUB), and Regional background (RB).

Table 1
List of air quality monitoring sites providing UFP-PNSD datasets for this study, including measurement periods, size range (in nm), and available ancillary pollutants. Categories include Urban Background (UB), Traffic (TR), Suburban Background (SUB), and Regional Background (RB); ND indicated not determined.

City (Country)	Station Name	Acronym	Period	Range	Ancillary pollutants
Antwerp (BE)	Borgerhout	ANT_UB	2017–2019	10–808	BC, PM_{10}, $PM_{2.5}$, SO_2, NO, NO_2, O_3
Athens (GR)	Thissio	ATH_UB	2015–2019	10–470	BC, PM_{10}, NO, NO_2, O_3, CO
Barcelona (ES)	Palau Reial	BCN_UB	2013–2019	12–478	BC, PM_{10}, $PM_{2.5}$, SO_2, NO, NO_2, O_3, CO
Budapest (HU)	BpART Lab	BUD_UB	2009–2019	11–816	PM_{10}, SO_2, NO, NO_2, O_3, CO
Dresden (DE)	Winckelmann Str.	DRE_UB	2010–2019	10–800	PM_{10}, SO_2, NO, NO_2, O_3
Granada (ES)	UGR	GRA_UB	2017–2019	11–496	BC, PM_{10}, SO_2, NO, NO_2, O_3, CO
Helsinki (FI)	SMEAR III	HEL_UB	2009–2019	10–708	SO_2, NO, NO_2, O_3, CO
Lecce (IT)	ECO Observatory	LEC_UB	2015–2019	10–800	BC, SO_2, NO, NO_3, O_3
Leipzig (DE)	TROPOS	LEI_UB	2009–2019	10–800	ND
London (GB)	North Kensington	LND_UB	2011–2018	17–604	BC, $PM_{2.5}$, SO_2, NO, NO_2, O_3, CO
Madrid (ES)	CIEMAT-Moncloa	MAD_UB	2013–2019	15–661	BC, PM_{10}, SO_2, NO, NO_2, O_3, CO
Mülheim an der Ruhr (DE)	Mülheim-Styrum	MUL_UB	2009–2019	14–496	PM_{10}, NO, NO_2
Rochester NY (US)	NYS DEC	ROC_UB	2011–2019	12–470	BC, $PM_{2.5}$, SO_2, NO, NO_2, O_3
Zurich (CH)	Kaserne	ZUR_UB	2015–2019	17–478	BC, PM_{10}, SO_2, NO, NO_2, O_3, CO
Dresden (DE)	North	DRE_TR	2009–2019	10–800	BC, PM_{10}, NO, NO_2, O_3
Helsinki (FI)	Mäkelänkatu	HEL_TR	2015–2019	11–800	BC, PM_{10}, $PM_{2.5}$, SO_2, NO, NO_2, O_3
Leipzig (DE)	Mitte	LEI_TR	2010–2019	10–800	BC, PM_{10}, SO_2, NO, NO_2
London (GB)	Marylebone Rd	LND_TR	2010–2019	17–604	BC, $PM_{2.5}$, SO_2, NO, NO_2, O_3, CO
Stockholm (SE)	Hornsgatan	STO_TR	2012–2018	10–410	PM_{10}, $PM_{2.5}$, NO, NO_2, CO
Athens (GR)	Demokritos	ATH_SUB	2010–2019	10–550	PM_{10}, NO, NO_2, O_3
Lille (FR)	Villeneuve d'Ascq	LIL_SUB	2017–2019	20–496	PM_{10}, NO, NO_2, O_3
Paris (FR)	SIRTA	PAR_SUB	2013–2019	11–800	BC, PM_1, NO, NO_2, O_3
Prague (CZ)	Suchdol	PRA_SUB	2012–2019	10–475	PM_{10}, $PM_{2.5}$, SO_2, NO, NO_2, O_3, CO
Ispra (IT)	JRC	IPR_RB	2016–2019	10–800	BC, PM_{10}, SO_2, NO, NO_2, O_3, CO

2.2. Positive matrix factorization

Positive Matrix Factorization (PMF; Paatero and Tapper, 1994) is the most recently used data analysis method to identify and apportion the sources of PNSD. It is a multivariate factor analysis tool that decomposes a matrix of speciated sample data into two matrices: factor contributions and factor profiles. These need to be interpreted to identify the source types using measured source profile information, and emissions inventories.

The increased use of PMF came as a result of the freely available implementation provided by the U.S. Environmental Protection Agency (US EPA; Norris et al., 2014). However, the current implementation of USEPA PMF 5.0 program, a graphic user interface coupled to the underlying solver, the multilinear engine 2 (ME-2; Paatero, 1999), does not handle datasets of more than approximately 500,000 data points. Thus, Hopke et al. (2023) developed a tool that would permit the PMF analysis of large datasets using ME-2, which is used in this study. A roadmap of the process of the PMF followed in this study is presented in Fig. 2.

The datasets included hourly averaged PNSD data combined with hourly concentrations of the ancillary pollutants available at each site, to help the identification of the sources. PMF requires individual uncertainty estimates for each data value. Uncertainties in the PNC values were estimated using the approach of Ogulei et al. (2007), Squizzato et al. (2019) and Hopke et al. (2024), calculated by:

$s_{ij} = \alpha_{ij} + C_3 \cdot n_{ij}$ where $\alpha_{ij} = 0.01(n_{ij} + \bar{n}_{ij})$ and C_3 is a constant determined by trial-and-error testing values between 0.001 and 0.15. The lowest and highest bins of the PNSD have been reported to have increased measurement error (Wiedensohler et al., 2018). Consequently, uncertainties for the 3 % lowest and 3 % highest size bins were multiplied by a factor of 2, and by a factor of 1.5 for the subsequent 3 % lower and 3 % higher size bins (Rivas et al., 2019).

Uncertainties for the ancillary pollutants were calculated following the methodology established by Polissar et al. (1998). An additional uncertainty K was applied to all the variables. The values of C_3 and K that optimise the model are presented in Table S2.

The datasets for each site were independently analysed by PMF. PMF was run multiple times for different numbers of factors (sources), from 3 to 7 factors. Then, the number of factors was finally determined examining the results and choosing the best solution. These best solutions were selected based on the accepted criteria and guidelines (Belis et al., 2019; Hopke et al., 2023), considering: (i) scaled residuals approximately randomly distributed between −3 and 3, (ii) a Q_{true}/Q_{exp} ratio close to 1, (iii) profile uncertainties determined by the displacement (DISP) method, and (iv) the provision of the most physically meaningful profiles and temporal behaviours.

To support the identification of the sources, the contributions of each factor to the variance of the co-located ancillary pollutants, daily patterns, seasonality and polar plots were evaluated. The data analysis and plots were performed with the R statistical software (v4.2.3, R Core Team, 2023) and the package *Openair* (Carslaw and Ropkins, 2012).

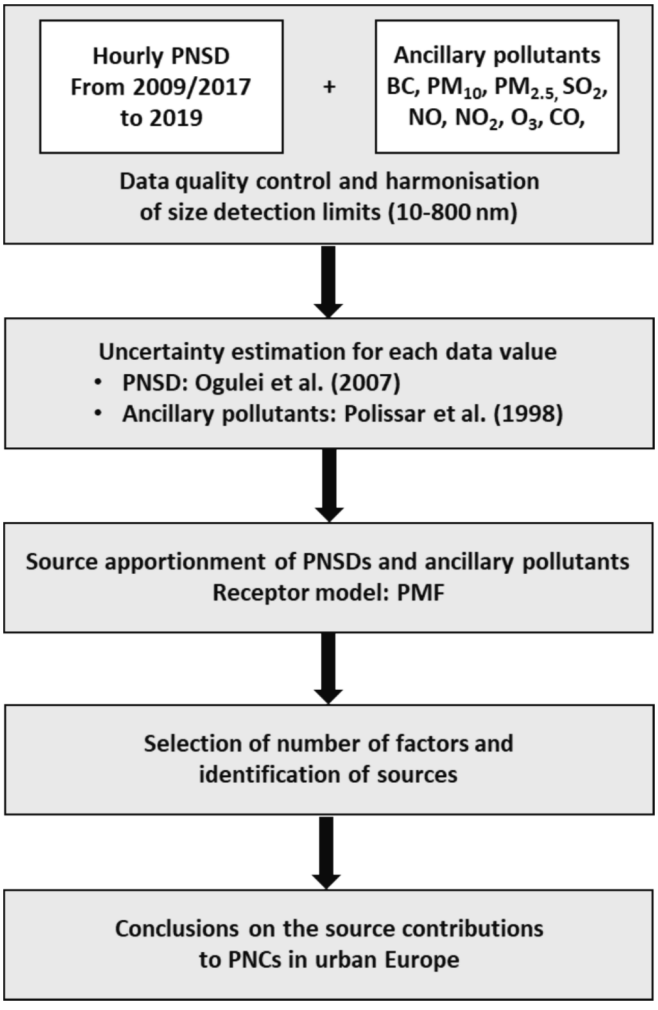

Fig. 2. Roadmap of the process followed for the source apportionment of PNSD using PMF.

2.3. Splitting of Nucleation into Photonucleation and traffic sources

At some sites, sources with prevalence in the Nucleation mode included particles generated by photonucleation processes, and those emitted from road traffic; and PMF was not able to separate them into two factors due to the similar PNSDs. Thus, these sources were split following a methodology developed by Rodríguez and Cuevas (2007) and Rivas et al. (2019). NO_X and BC were used as proxies for traffic emissions (see Table S3). Considering that the morning concentration peak of this source is built mostly by primary traffic particles, NO_X or BC concentrations were multiplied by a scaling factor so it matched the PNC of this source at morning peak hour. This scaling factor (the ratio between the PNC of the source and the proxy) was calculated for each day. The percentile 10 % of the PNC of this source/BC or NO_X at morning traffic rush hours at each site was selected as a scaling factor. The selection of the 10th percentile was based on previous studies (Rodríguez and Cuevas, 2007; Reche et al., 2011; Kulmala et al., 2016; Kalogridis et al., 2018; Nie et al., 2022) and the variability of PNC of each year of data in this study. Also, at some sites, all the particles from photonucleation were attributed to traffic sources during the night hours, as no photonucleation would be expected since these particles are formed due to solar radiation. Examples of the splitting (DRE_UB and MUL_UB) are shown in Figures S1 and S2.

2.4. Trend analysis

Inter-annual trend analysis of the source contributions was conducted using the same methodology as described by Garcia-Marlès et al. (2024). For detection of monotonic trends, datasets covering at least 4 complete years within a period of more than 5 years were analysed using the non-parametric Theil-Sen method (Sen, 1968; Theil, 1992), a widely used approach for air quality trend assessments (Carslaw and Ropkins, 2012). Monthly averages were calculated with a threshold of 30 % of the hourly concentration data. The Theil–Sen slope, which represents the median of all the possible slopes between data pairs, was used to quantify the magnitude of the trends, while statistical significance (ss) was evaluated using the *Openair* R package (Carslaw and Ropkins, 2012).

A random effects *meta*-analysis was performed on the estimated trends for each source, using individual slopes expressed as percentage changes per year along with their 95 % confidence intervals. The mean

effect was calculated separately for site type (urban, suburban, and traffic) as well as for all sites combined. The analysis was conducted using the *meta* R package (Balduzzi et al., 2019).

3. Results and discussion

3.1. Sources identified

From 4 to 7 factors of PNC were identified at each site. In total, 10 different factors were found associated to different aerosol sources for the 24 datasets of the study: *Traffic-1*, *Traffic-2*, *Mixed traffic*, *Traffic-Nucleation*, *Photonucleation*, *Urban background*, *Domestic heating*, *Regional-1*, *Regional-2* and *Long-distance transport*. However, in some cases a general nucleation factor (<25 nm) obtained by PMF was further split into *Photonucleation* and *Traffic-Nucleation* (see Table S3). In other cases, a coarser factor (25–35 nm) associated with traffic was split into *Traffic-1* and *Photonucleation*. The *Photonucleation* source was then added to the existing *Photonucleation* source obtained directly from PMF at the site. This additional source is linked to particles generated by photochemical processes but with a regional origin, as evidenced by the coarser size mode and its peaks at midday, albeit with a delay compared to a local photonucleation.

The sources identified at each site are characterised by different PNSDs and trends. Modes' sizes with the highest PNC for the different sources at each site are reported in Table 2. These modes are affected by the size ranges of each site, thus the lower detection limit has to be considered, especially in the nucleation sources. Results of the source apportionment for each site are interpreted in Supplementary text T1 and presented in Figures S3-S77 and Tables S4-S27. These show the profiles for PNSD, the contributions to the variance of ancillary pollutants, daily, monthly and weekly trends of PNC, and polar plots.

3.1.1. Traffic sources

Four different factors associated with road traffic source were identified at the sites of this study, with similar temporal behaviours but different PNSDs (Table 2; Fig. 3). *Traffic-1* and *Traffic-2* are typically documented in the existing literature (Hopke et al., 2022).

Traffic-1 identified in this study is characterised by major size modes with peaks ranging between 23 and 39 nm (Table 2). This size mode associated to traffic is commonly attributed to gasoline vehicle emissions in ambient air urban PNSD measurements (Ogulei et al., 2007; Liu et al., 2014; Hopke et al., 2022, 2024; Vörösmarty et al., 2024), freshly emitted traffic particles on nearby roads (Gu et al., 2011), or nucleation of particles generated during dilution of diesel exhaust semi-volatile organic compounds (SVOCs) (Harrison et al., 2011, Damayanti et al., 2023). ***Traffic-2*** is characterised by size mode peaks at 55–119 nm (Table 2), and is associated with primary diesel vehicle emissions (Ogulei et al., 2007; Liu et al., 2014; Hopke et al., 2022). Some studies also suggest that this larger traffic mode is due to the coagulation of the particles moving from the sources, i.e., an aged traffic emission (Zhu et al., 2002; Gu et al., 2011). The traffic origin of both factors is supported by peaks observed during rush hours in the morning and evening, lower values in summer in cities where the car fleet decreases on holidays, and low weekends PNCs (Fig. 3). Also, these have mainly a local origin and predominate at low wind speeds (Supplementary text T1). However, a few cities, such as Antwerp, Leipzig, Paris, Rochester or Stockholm, have higher total PNC in summer, and most of the source contributions are also higher in summer, probably due to meteorological conditions favouring more stagnation in summer (Hopke et al., 2024). *Traffic-2* profiles exhibit higher contributions to the variance of BC and NO_X compared to *Traffic-1* (Supplementary text T1). This aligns with interpretations, as diesel exhaust emits BC-rich soot particles when not equipped with diesel particle filters (DPFs) (Damayanti et al., 2023, and references therein) and is responsible for most of the traffic-related NO_X emissions (He et al., 2015). Both profiles also contribute to CO, with *Traffic-2* additionally contributing to PM_X.

Mixed traffic is characterised by major size mode peaks at 43–55 nm (Table 2), falling within the range between *Traffic-1* and *Traffic-2*. It represents a highly traffic-influenced urban background; thus, it is mixed with other sources, keeping the daily, seasonal and weekly patterns of traffic sources (Fig. 3). This factor also predominates at low wind speeds and has contributions to the variance of BC, NO_X and CO (Supplementary text T1).*Traffic-1* and *Traffic-2* were well separated and identified at all the UB and TR sites except for ATH_UB, BUD_UB and both sites in Helsinki (HEL_UB and HEL_TR). These factors were also identified in ATH_SUB and PAR_SUB, but not at the other SUB and RB sites. The sites where these factors were not individually identified presented the *Mixed traffic* factor, but the three distinct traffic factors

Table 2
Size modes with the highest PNC of the sources identified in each site. In parentheses, size mode of lower peaks in the PNSD. TR-Nucl, Traffic-Nucleation; TR-1, Traffic-1; Mixed TR, Mixed traffic; TR-2, Traffic-2; Photonucl., Photonucleation; UB, Urban background; Dom heat, Domestic heating; Reg-1, Regional-1; Reg-2, Regional-2; LDT, Long-distance transport.

Station	TR-Nucl.	TR-1	Mixed TR	TR-2	Photonucl.	UB	Dom heat	Reg-1	Reg-2	LDT
ANT_UB	11	39		83	11			271 (30)	191 (10)	
ATH_UB		28	47		16	160 (28)	84			
BCN_UB		27	43	88	13				151 (31)	300 (69, 13)
BUD_UB	20		52		20	114		250 (114, 39)	169 (16)	
DRE_UB		28	54	119	11			291	232 (48)	
GRA_UB	13	23	43	98	13			175 (27)		
HEL_UB	16		45					200 (28)	80	
LEC_UB	11	27		60	11		106	260	48 (208)	
LEI_UB	13	28	54	106	13			364 (95, 14)	232	
LND_UB		37		87	22			255 (65)		
MAD_UB	19	37		69	19	188 (24)			151 (20)	
MUL_UB	15	29	50	88	15	188 (36)		322 (78, 19)		
ROC_UB	18	35		67	18		41	246 (20)	249	
ZUR_UB		31		55	20		106	300 (31)	188 (32)	
DRE_TR	16	38		85	16			260 (28)	208 (28)	
HEL_TR	13		55					213 (11)	30 (176)	
LEI_TR	14	39		95	14			291 (25)		
LND_TR	19	34		81				87 (255)		
STO_TR	17	35		79				198		
ATH_SUB		34		70	12				178 (25)	
LIL_SUB	24		51		24	106		269 (74)	46 (188)	
PAR_SUB		28		74				199	104	
PRA_SUB			45		16		82	195 (32)		
IPR_RB			45		18		99	198	36 (198)	

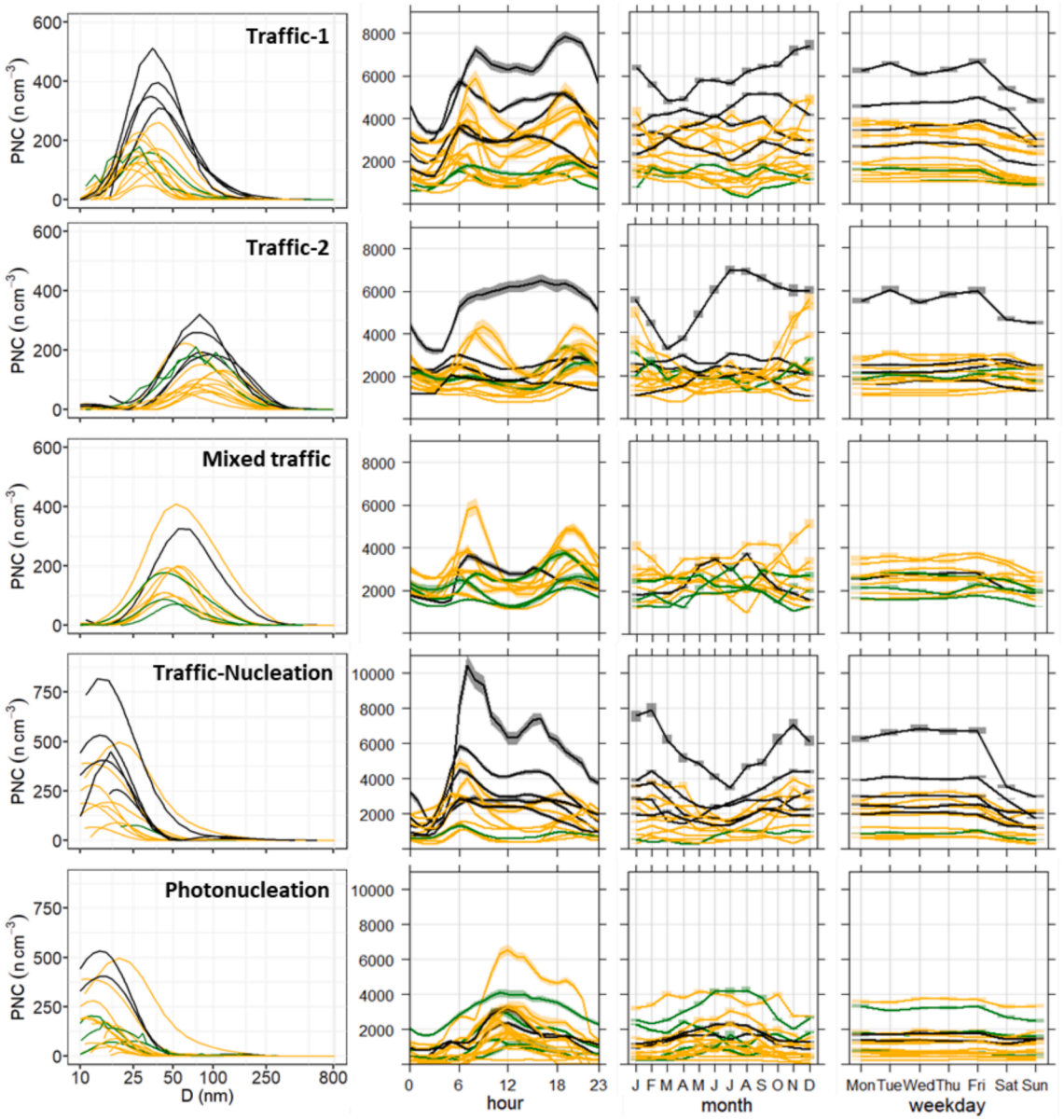

Fig. 3. Particle number size distribution (PNSD) profiles and daily, monthly and weekly patterns of *Traffic-1*, *Traffic-2*, *Mixed traffic*, *Traffic-Nucleation*, and *Photonucleation* sources across all sites. Urban background (UB) sites are denoted in yellow, Traffic (TR) sites in black, and Suburban background (SUB) and Regional background (RB) sites in green. (For interpretation of the references to colour in this figure legend, the reader is referred to the web version of this article.)

were identified at several UB sites (BCN_UB, DRE_UB, GRA_UB, LEI_UB and MUL_UB). The absence of separate identification of *Traffic-1* and *Traffic-2* at some sites may be attributed to aerosol dynamical processes affecting ultrafine particles during transport and air mass recirculation, which results in the mixing of particles from different origins (Hamed et al., 2007; Junkermann and Hacker, 2018; Lv et al., 2020). Due to the collinearity of temporal patterns in particles emitted by road traffic, PMF struggles to distinguish these two sources, especially at suburban sites.

Traffic-Nucleation is characterised by size mode peaks at 11–20 nm (Table 2), falling into the lowest size bins. The differences in modes between the sites are linked to the lower size detection limit, affecting the Nucleation mode PNC. This traffic exhaust factor is associated to the nucleation of the particles immediately after the emission of SVOCs (from a mixture of those arising from the regeneration of DPF in diesel vehicles and from catalytic converters in gasoline ones) to the atmosphere as they dilute and cool, leading to NPF (Harrison et al., 2011; Mamakos and Martini, 2011; Trechera et al., 2023; Saarikoski et al., 2024). It also follows the daily, seasonal and weekly patterns of traffic sources (Fig. 3) and predominates at low wind speeds (Supplementary text T1). This factor was identified at most sites after applying the methodology to split the factor from *Photonucleation* (see methodology) (ANT_UB, BUD_UB, GRA_UB, LEC_UB, LEI_UB, MAD_UB, MUL_UB, ROC_UB, DRE_TR, LEI_TR and LIL_SUB). At other sites, it was identified directly from PMF (HEL_UB, HEL_TR, LND_TR and STO_TR). Furthermore, it has been shown that *Traffic-Nucleation* increases with decreasing ambient temperature. Weichenthal et al. (2008) found a decrease of around 10,000 # cm^{-3} per each increase of 10 °C, at sites close to traffic emissions.

3.1.2. *Photonucleation*

Photonucleation is characterised in this study by size modes with peaks ranging between 11 and 22 nm (Table 2) and represents most of the PNCs in the Nucleation mode at urban sites. As mentioned above, the lower size detection limit influences the profiles at each site. This source is associated with photochemically induced NPF events, which are

enhanced by high insolation (Kulmala and Kerminen, 2008; Brines et al., 2015). Thus, peaks at midday/late morning are observed across all sites, and PNCs are higher in summer, coinciding with peak solar radiation (Fig. 3). At certain sites, BCN_UB as an example (see Supplementary text T1), smaller peaks during traffic rush hours in the morning and evening persist. This result suggests that the source still includes Nucleation mode particles from traffic exhaust even after applying the methodology to distinguish photonucleation particles from traffic nucleation particles. While traffic-related pollutants are not prominent in the *Photonucleation* source, elevated levels of SO_2 and O_3 are observed at most sites (Supplementary text T1). This source was identified at all sites except for HEL_UB, HEL_TR, LND_TR, STO_TR and PAR_SUB. However, for the latter, photonucleation particles are present in the source identified as *Regional-2*.

Photonucleation particles are formed in high-insolation and high wind speed environments, leading to NPF events (Kulmala and Kerminen, 2008; Brines et al., 2015; Salma et al., 2021; Trechera et al., 2023; among others). These events are further enhanced by a low condensation sink (McMurry and Friedlander, 1979), occurring when traffic exhaust emissions decrease, and with available SO_2. At some sites such as BCN_UB, it is mostly influenced by nucleated particles in the high SO_2 plumes emitted from the harbour, as supported by winds blowing from that direction and a previous analysis of cluster ions by Nitrate Chemical Ionisation Atmospheric Pressure interface Time of Flight Mass Spectrometer (CI-APi-ToF) (Brean et al., 2020). Additionally, coal-fired power plants emitting SO_2 contribute to NPF episodes at other sites, especially in central Europe (Junkermann et al., 2011). These are generally transported at high altitudes. Insolation and associated convective dynamics lead to the growth of the mixing layer, which traps these plumes and causes Hewson-type fumigations (of these high

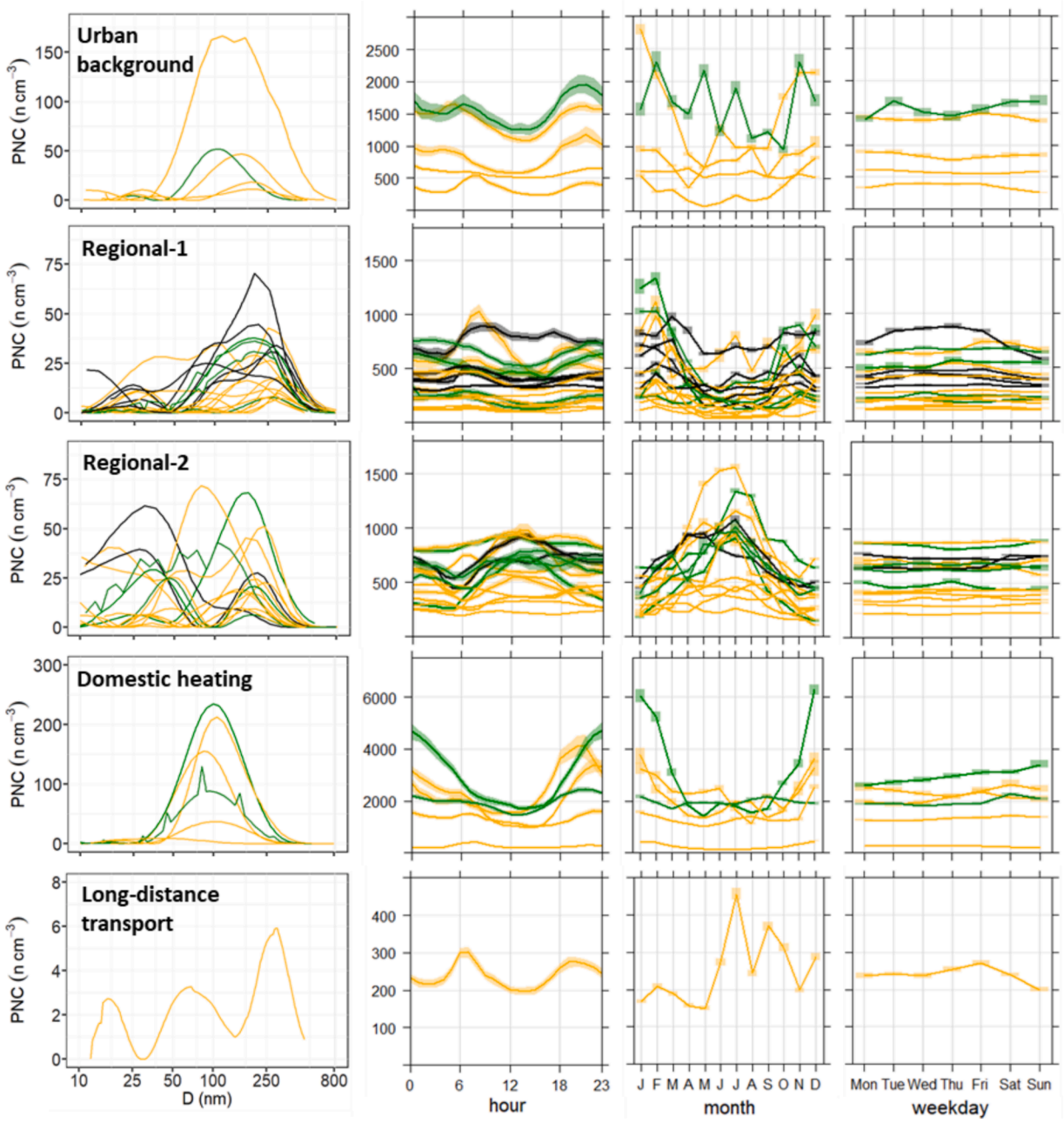

Fig. 4. Particle number size distribution (PNSD) profiles and daily, monthly and weekly patterns of *Regional-1*, *Regional-2*, *Urban background*, *Domestic heating* and *Long-distance transport* sources across all sites. Urban background (UB) sites are denoted in yellow, Traffic (TR) sites in black, and Suburban background (SUB) and Regional background (RB) sites in green. (For interpretation of the references to colour in this figure legend, the reader is referred to the web version of this article.)

Nucleation mode particles) on the surface (Hewson, 1955). Furthermore, regional-scale nucleation episodes might account for a high proportion of NPF (Kalkavouras et al., 2020).

3.1.3. Urban and regional background

Urban background is characterised by size modes peaks at 106–188 nm (Table 2) and follows similar traffic patterns with the highest values at rush hours and during winter (Fig. 4). It has high contributions of PM_X, BC, NO_X and CO and has a local origin (Supplementary text T1). This source, which was identified at ATH_UB, BUD_UB, MAD_UB, MUL_UB and LIL_SUB, can be described as highly traffic influenced urban background, following similar traffic profiles and patterns but with a coarser mode. It includes aged traffic particles that had grown after the emission, with a high amount of carbon agglomerates supported by the high contributions of BC (Beddows et al., 2015; Rivas et al., 2019). It is differentiated from the *Mixed-traffic* source only because of the coarser size mode of the *Urban background.*

Two different regional sources were identified due to opposite day-night and summer-winter patterns. The ***Regional-1*** is characterised by a multimodal distribution with main peaks ranging between 175–364 nm and secondary peaks in the Aitken and Nucleation modes (Table 2). It is higher at night and during winter (Fig. 4), and has high contributions of PM_X and traffic-related pollutants. It is associated with high wind speeds (usually easterly winds in northern and central Europe) but has also a local origin (especially in southern and eastern Europe) (Supplementary text T1). The ***Regional-2*** profiles also display a multimodal distribution but with finer size modes, with main peaks ranging between 80–232 nm (Table 2). It has higher PNCs at midday and during summer (Fig. 4), coinciding with higher insolation. It has high contributions of PM_X, O_3 and SO_2, and is associated with high wind speeds (Supplementary text T1). Neither of these sources exhibits a day-of-the-week pattern.

Regional-1 is mainly associated with nitrates, which are primarily formed through atmospheric oxidation of NO_X (Seinfeld and Pandis, 2016). This mainly occurs during winter, as ammonium nitrate evaporates in summer due to high temperatures, and at night, consistent with semi-volatile nitrate condensing on locally emitted particles during periods of lower temperature and higher relative humidity (Dall'Osto et al., 2009; Masiol et al., 2016). The particles in the Nucleation and Aitken mode are likely associated with the gas-to-particle conversion of local NO_X emissions whereas the Accumulation mode particles are formed during the transport and reactions of their precursor gases, NH_3 and NO_X (Kasumba et al., 2009; Squizzato et al., 2019). Furthermore, domestic emissions of UFP (higher in winter and night) might also contribute to this source.

Regional-2 is usually associated with secondary ammonium sulphate and organic aerosols. The high summer insolation (and O_3 concentrations) accelerates the oxidation of SO_2 and VOCs to produce NPF with an origin from H_2SO_4 reaction with NH_3 or amines, with a subsequent growth dominated by condensation of oxidised VOCs (Ehn et al., 2014). The ageing of these particles to build up the regional background yields a coarser size fraction. This is enhanced in the summer season, because of the higher insolation and O_3, but also biogenic VOC emissions. It has a finer PNSD than the *Regional-1* because of the high contributions of NPF followed by growth, and because of the thermal instability of ammonium nitrate in summer but not in winter. Several sites (LEC_UB, HEL_UB, HEL_TR, LIL_SUB and IPR_RB) show the main peaks of this source in the Aitken mode between 30–80 nm, along with additional peaks in the Accumulation mode. These mainly consist of nucleated particles that have grown during transport from the emission sources, especially associated with SO_2-rich plumes (Qian et al., 2007; Bousiotis et al., 2019). In the Western Mediterranean, the well-known summertime vertical recirculation of air masses (Millán et al., 2000; Gangoiti et al., 2001) is a major cause of regional O_3 pollution episodes. It also contributes to the enrichment of aerosol particles and their precursors, leading to higher levels of UFPs in *Regional-2* compared to *Regional-1* (Carnerero et al., 2019).

3.1.4. Other sources

Domestic heating is characterised by size modes ranging between 82–106 nm in ATH_UB, LEC_UB, ZUR_UB, PRA_SUB, and IPR_RB, and a wide PNSD profile in ROC_UB, where the maximum PNC occurs at 41 nm (Table 2). It is higher at night, during winter, and at weekends (Fig. 4), when domestic burning is more frequent (Kleeman et al., 2009; Gu et al., 2011; Corsini et al., 2019), and has high contributions of BC and CO (Supplementary text T1). BC and CO are emitted as products of incomplete combustion of carbon-containing fuels, such as wood and coal (Wei et al., 2012; Chen et al., 2015). Significant emissions of UFP have been reported from these domestic combustion processes (Tiwari et al., 2014; Zhang et al., 2014; de la Sota et al., 2018; Wang et al., 2020; Kuye and Kumar, 2023). These sources include cooking and heating activities, emitted by wood-burning and pellet stoves, fireplaces, electric heaters, and kitchen stoves, among others. Additionally, PNC peaks in spring and summer could be attributed to biomass burning resulting from agricultural activities and fires (Cesari et al., 2018). However, in some sites such as GRA_UB, HEL_UB, HEL_TR, and ATH_SUB, this source was not individually identified by PMF, but contributions of domestic heating might be included in traffic sources, especially in Traffic-2, with higher contributions at night. For a campaign in winter 2015–2016 in GRA_UB, Casquero-Vera et al. (2021) found that primary biomass burning contributed 9 % of total PNC, but PMF was not applied.

Long-distance transport was only identified in BCN_UB and is characterised by a multimodal distribution with the main size mode at 300 nm (Table 2). Higher PNCs coincide with rush hours and during summer (Fig. 4), with high contributions of PM_X. It is mainly associated with particles from the Sahara Desert in Africa, as shown by the high contributions observed with SW winds with high velocities, and back-trajectory analyses (Supplementary text T1). A similar PNSD was found by Al-Dabbous and Kumar (2015) for a long-range transport source associated with Arabian dust events. However, lower contributions with a local origin are also observed, related to road dust emitted from traffic, explaining the diel pattern (Gu et al., 2011). Additional sources contributing might include long-range transport of polluted air masses (with high loads of sulphate and other secondary pollutants) and forest fires. Figures S12 illustrates the mean Dust Surface Concentration on days characterised by substantial dust contributions in Barcelona, coinciding with documented dust events. During these periods, elevated levels of sulphate particles (Figure S13) and emissions from forest fires (Figure S14) were also recorded. However, this source was not identified by PMF in GRA_UB, MAD_UB or LEC_UB, which might also have significant contributions from Saharan dust.

3.2. Quantitative source contributions

Fig. 5 shows the relative contribution to average PNCs of the sources identified at each study site. The sum of all the traffic contributions (*Traffic-1*, *Traffic-2*, *Mixed traffic* and *Traffic-Nucleation*) represents 70–88 % of the average PNC at 9 out of the 14 UB sites analysed, and 47–61 % at the remaining 5 sites. As it could be expected, at TR sites, traffic sources contribute even more significantly, accounting for 77–95 % of the average PNC. These contributions are higher at TR compared to UB sites in cities where PNC measurements are conducted at both types of sites. It is notable that *Traffic-Nucleation* is more relevant at TR sites (16–54 % of the average PNC at the 5 studied sites) compared to UB sites (7–38 % of the average PNC identified at 9/14 sites). Traffic nucleated particles might arise from gasoline emissions and, to a larger extent, from SVOCs escaping the DPFs in diesel vehicles (Harrison et al., 2011, Damayanti et al., 2023). These traffic particles exhibit rapid growth as they move away from the traffic source, thus at UB sites, traffic particles are generally coarser than in other traffic factors. This effect arises from coagulation and from loss of the delayed nucleated diesel traffic mode by evaporation as they move into cleaner background air (Dall'Osto

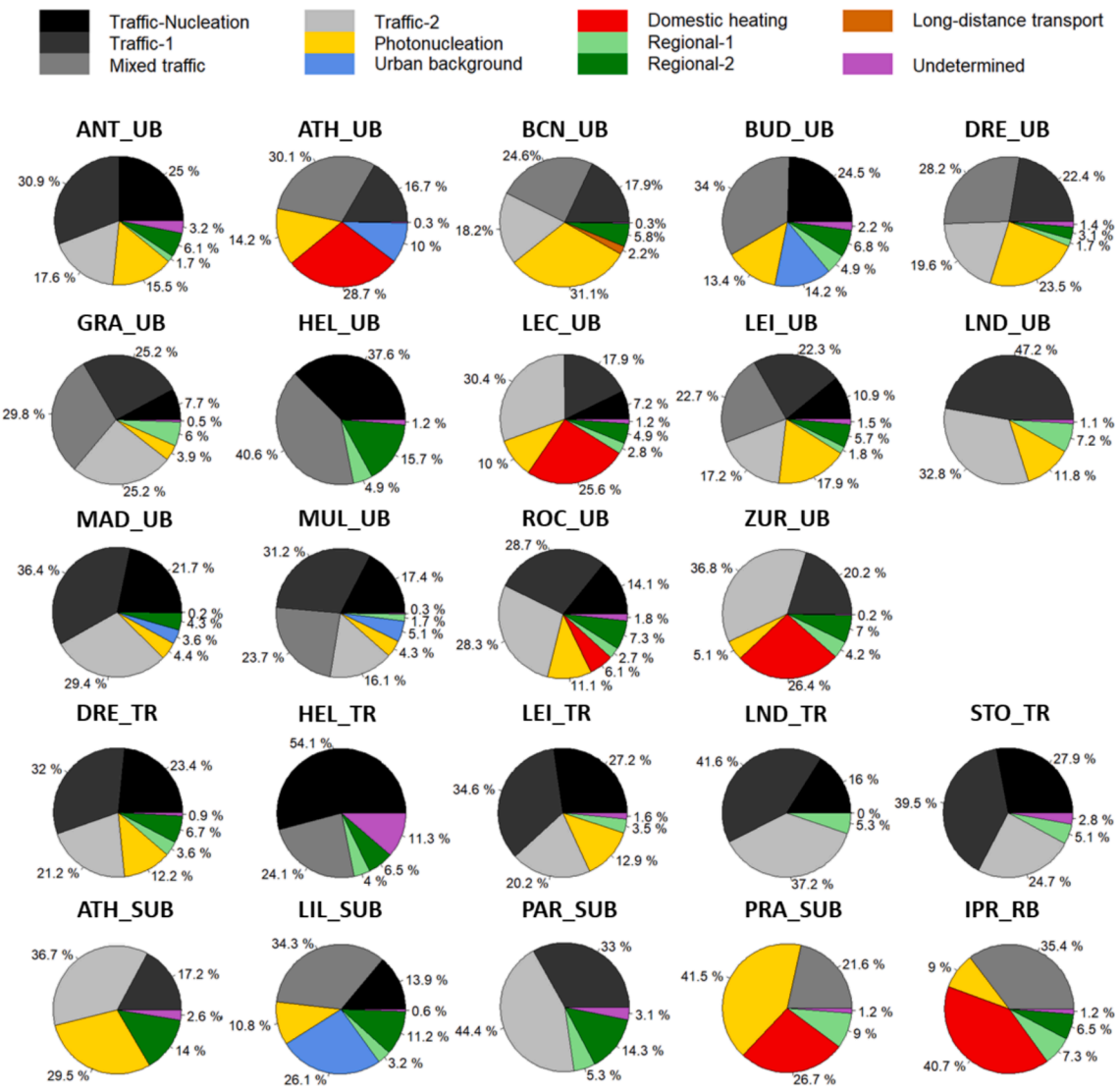

Fig. 5. Relative contributions (%) of particle number concentration (PNC) from the identified sources at each study site. The *Undetermined* category (in purple) represents the fraction of PNC not assigned to a specific source by PMF. (For interpretation of the references to colour in this figure legend, the reader is referred to the web version of this article.)

et al., 2011; Harrison et al, 2016). However, it is important to note that at sites where the splitting methodology of nucleated particles was applied, the uncertainty in quantifying source contributions might be higher. Additionally, the contribution of the traffic sources may contain particles from other (less relevant) sources and be affected by the distance from the monitoring site to major roads or by specific climate/meteorological patterns of the cities. Moreover, at sites like HEL_TR, the PMF analyses resulted in regional source profiles with traffic patterns that were not possible to split into traffic/background portions, potentially leading to an underestimation of traffic contributions. At SUB and RB sites, traffic contributions are not consistently the major contributors across all locations, comprising 22–77 % of the average PNC, with PAR_SUB exhibiting the highest traffic contributions among these sites.

Accordingly, the results point to road traffic as the major contributor to UFP/PNC in urban Europe. The high contribution from traffic emissions to total PNSD has also been reported in literature for many urban environments around the world (Pey et al., 2009; Dall'Osto et al., 2012; Liu et al., 2014; Beddows et al., 2015; Brines et al., 2015; Sowlat et al., 2016; Rivas et al., 2019; Squizzato et al., 2019; Kalkavouras et al., 2024, and others).

Following traffic, *Photonucleation* is a significant contributor at several sites, primarily driven by NPF mostly at regional scales. In BCN_UB, with relatively high insolation levels compared with other study cities (Trechera et al., 2023), this source contributes 31 % to the average PNC, notably higher during summer, but remaining significant throughout the year. As stated above, this is highly influenced by emissions of precursors from shipping. Dresden and Leipzig also exhibited substantial contributions from *Photonucleation*, accounting for 24 % (UB) and 12 % (TR) in Dresden, and 18 % (UB) and 13 % (TR) in Leipzig. Also, as stated above, these values were probably caused by surface fumigation by higher-altitude atmospheric layers (enriched in Nucleation mode particles through NPF processes) during the growth of the planetary boundary layer (Junkermann et al., 2016). This source was identified at all remaining UB sites (4–16 % of the average PNC), except for Helsinki. Additionally, it was present at all SUB and RB sites except for PAR_SUB, with the highest contribution observed at PRA_SUB. The contributions of this source may be subject to under or overestimation at sites where the nucleation splitting (traffic/photonucleation) methodology was applied.

Domestic heating contributed significantly at ATH_UB, LEC_UB, ZUR_UB, PRA_SUB, and IPR_RB (26–41 % of the average PNC) and less at ROC_UB (6 %). However, this source probably contributed also to

Regional-1, Urban background and traffic factors at sites where *Domestic heating* was not identified.

Lower contributions were observed for *Urban background* (4–14 % of the average PNC at 4/19 UB and TR sites, and 26 % at the SUB site in Lille), *Regional-1* (2–9 % at 20/24 sites), *Regional-2* (3–16 % at 16/24 sites) and *Long-distance transport* (2 % in BCN_UB). However, these contributions are also affected by other sources such as traffic.

3.3. Inter-annual trends of source contributions

Following the study by Garcia-Marlès et al. (2024), which evaluated long-term trends of UFP/PNC concentrations of most of the sites of this study, inter-annual trends of contributions of sources identified in this study were evaluated. Sites included for the trend analysis, that provide more than 4 complete years in a period longer than 5 years, are: BCN_UB, DRE_UB, HEL_UB, LEI_UB, LND_UB, MUL_UB, ROC_UB, DRE_TR, HEL_TR, LEI_TR, LND_TR, STO_TR, ATH_SUB and PRA_SUB.

Total traffic emissions (the sum of all the traffic factors) decreased with statistically significant (ss) trends at 10/14 sites, including 5/5 traffic sites and 5/6 European UB sites (Fig. 6). *Total traffic* decrease, in terms of PNC, −578, −148 and −42 # cm^{-3} yr^{-1} for the TR, UB and SUB sites, respectively. The *meta*-analysis yielded ss trends for UB (−2.15 [-4.17; −0.13] % yr^{-1}), TR (−5.40 [-7.66; −3.13] % yr^{-1}) and all sites (−3.26 [-4.78; −1.75] % yr^{-1}). The highest decrease of the traffic factors was observed in *Traffic-2* (diesel), with ss decreasing trends at 9/11 sites (−4.21 [-5.60; −2.83] % yr^{-1}, for the global *meta*-analysis), and a non-ss decrease at 1/11 site. *Traffic-1* decreased with ss trends at 5/11 sites (−2.78 [-4.78; −0.78] % yr^{-1}, for the global *meta*-analysis) and with non-ss decreasing trends at 4/11 sites. *Mixed traffic* decreased with ss trends at 4/7 sites (−2.61 [-4.46; −0.76] % yr^{-1}, for the global *meta*-analysis) and *Traffic-Nucleation* decreased with ss trends at 4/9 sites (−2.97 [-5.77; −0.16] % yr^{-1}, for the global *meta*-analysis).

Thus, PNCs from traffic sources decreased at most sites (all traffic sites and all UB European sites except LEI_UB), most probably as a consequence of the implementation of emission standards on European air quality, particularly EURO 5 and 6 (for cars) and V and VI (for heavy-duty vehicles) and other local measures that might have been implemented for road traffic. The highest significant decrease for *Traffic-2* (primarily associated with diesel vehicle emissions) aligns with the requirement of EURO 5 and V for diesel vehicles to be equipped with DPF (Damayanti et al., 2023). This result is consistent with the downward trends of BC, and the Aitken and Accumulation mode particles observed by Garcia-Marlès et al. (2024). However, Chen et al. (2022) and Damayanti et al. (2023) reported that the abatement effect of DPF of the Nucleation mode particles was minimal because DPFs do not retain SVOCs emitted by diesel cars and these nucleate leading to delayed primary particles. Supporting this effect, traffic factors of finer UFP fractions, *Traffic-Nucleation* and *Traffic-1*, decreased less at most sites, and in some cases, lost the ss. Furthermore, the reduction of sulphur (S) content in diesel might have contributed to reducing UFP from road traffic. However, ultra-low-S diesel (ULSD) was implemented in 2006 in Europe and the US (Hopke et al., 2024), which was before the period covered by the datasets in this study. Other road traffic policy measures, such as Low Emission Zones (LEZ) in many cities and the Congestion Charge in some of them, also might have contributed to this reduction (Patel et al., 2023).

ROC_UB is the only site that showed a ss increasing trend for traffic sources (+4.36 [1.39; 8.36] % yr^{-1}, for *Total traffic*), with the highest increase in *Traffic-Nucleation*. Hopke et al. (2024) found compatible results for this US city. They reported a decrease in traffic-related UFP from 2006 to 2012 (attributed to the implementation of Tier 2 standards), followed by a flat evolution and an increase in 2017–2019. They suggested rise in economic activity beginning in 2017 (higher HDD vehicle traffic) as the major cause of this increase, but also a possible leak from ageing DPFs (Preble et al., 2019).

Different trends for *Photonucleation* among the sites evaluated were observed, with ss increasing trends at 4/10 sites, non-ss trends at 6/10 (Fig. 6). The *meta*-analysis yielded a non-ss increasing trend for all sites. The increases might be linked to a reduction in condensation sink potential, which facilitates photochemical new particle formation (Spracklen et al., 2010; Kulmala et al., 2017). Trends for this source are expected to vary because of the different causes of NPF caused by photonucleation. Thus, as reported above, in some places this can be attributed to regional nucleation, in others to the impact of plumes of SO_2-emitting coal or fuel–oil power plants, and shipping emission plumes. All these sources of precursors and atmospheric processes affect specific cities and might have had different trends in the different cities. Furthermore, there is a ss increasing trend for temperature in these cities (Garcia-Marlès et al., 2024) that might have also influenced the increase of UFP from NPF in specific regions.

Urban background decreased with ss at the only site evaluated (MUL_UB), showing a rate of −3.59 [-4.52; −2.53] % yr^{-1} (Fig. 7). This is consistent with the decreasing trends of traffic sources because of the influence of traffic emissions in *Urban background*.

Regional-1 significantly decreased at most of the sites, with ss decreasing trends at 7/11 sites and non-ss trends at the remaining sites. The *meta*-analysis yielded a ss decreasing trend for all sites with an average rate of −5.40 [-7.36; −3.43] % yr^{-1} (Fig. 7). This change is probably associated with the decrease of primary PM emissions and precursors of UFP (SO_2, NO_X, and in less proportion VOCs and NH_3) across Europe, as reported by EEA (2023).

Regional-2 also showed a ss global decreasing trend (−1.90 [-3.56; −0.25] % yr^{-1}) but only decreased with ss at 2/8 sites (Fig. 7). This summer source was dominated by secondary sulphate and secondary organic aerosols where formation increased with insolation. In spite of the above observed decreased emissions of SO_2, the lower decrease of NH_3 and VOCs, but especially the increase of O_3 in urban environments (Sicard et al., 2021) might have prevented more marked decreases of this contribution compared with the winter one. Thus, the increase of ozonolysis reactions might have yielded to an increase in the formation of secondary particles in summer. Saiz-Lopez et al. (2017) reported that in Madrid the urban increase of O_3 resulted in an increase of 60–100 % of oxidising radicals, yielding in an increase of the potential of formation of secondary inorganic and organic particles.

Domestic heating did not show global ss trends, as only two sites (ROC_UB and PRA_SUB) had enough data for the trend analysis, making it difficult to reach any conclusions. *Long-distance transport* did not show ss trend for BCN_UB.

4. Conclusions

This study identified and quantified source contributions of ultrafine particles (UFP) and evaluated long-term trends of these source contributions, based on 24 particle number size distribution (PNSD) datasets from 18 cities in Europe and 1 in the USA. These locations included 14 urban background (UB), 5 traffic (TR), 4 suburban background (SUB), and 1 regional background (RB) sites.

Ten different factors are identified contributing to UFP-PNSD (*Traffic-1*, *Traffic-2*, *Mixed traffic*, *Traffic-Nucleation*, *Photonucleation*, *Urban background*, *Domestic heating*, *Regional-1*, *Regional-2* and *Long-distance transport*), with road traffic being the major contributor at all UB and TR sites (56–95 %). *Photonucleation* is also a significant contributor at many sites (4–41 % in 16/19 cities), primarily driven by new particle formation (NPF). These cities include not only those with high insolation from southern Europe, but many from central Europe. The causes of these high contributions of NPF are diverse (shipping, plumes from combustion plants, regional nucleation).

The results showed a clear reduction in UFP traffic ambient concentrations. These trends reached statistically significant decreases for *Total traffic* (the sum of all the traffic contributions) of −5.40 and −2.15 % yr^{-1} for TR and UB sites, respectively, or, in terms of PNC, of −578 and −148 # cm^{-3} yr^{-1}. This UFP abatement is most probably due to the

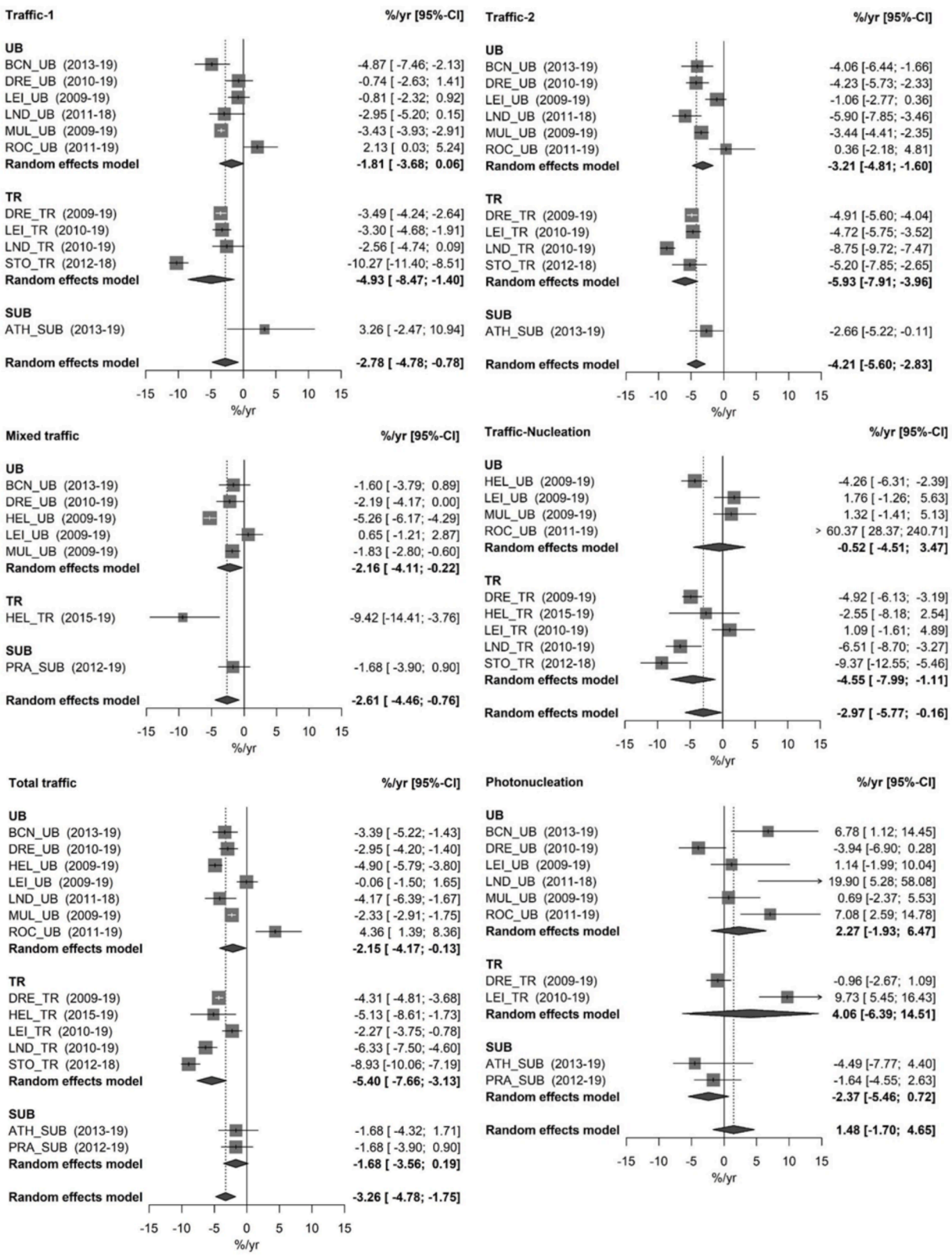

Fig. 6. Trend analysis and *meta*-analysis results for *Traffic-1*, *Traffic-2*, *Mixed traffic*, *Traffic-Nucleation*, *Total traffic* and *Photonucleation* sources. Trends are calculated using the Theil-Sen method. Mean effects for each site type (Urban background, UB; Traffic, TR; Suburban background, SUB; and Regional background, RB) are estimated using a random effects model. The *meta*-analysis results are presented for each pollutant across the different site types, as well as for global trends (dashed line).

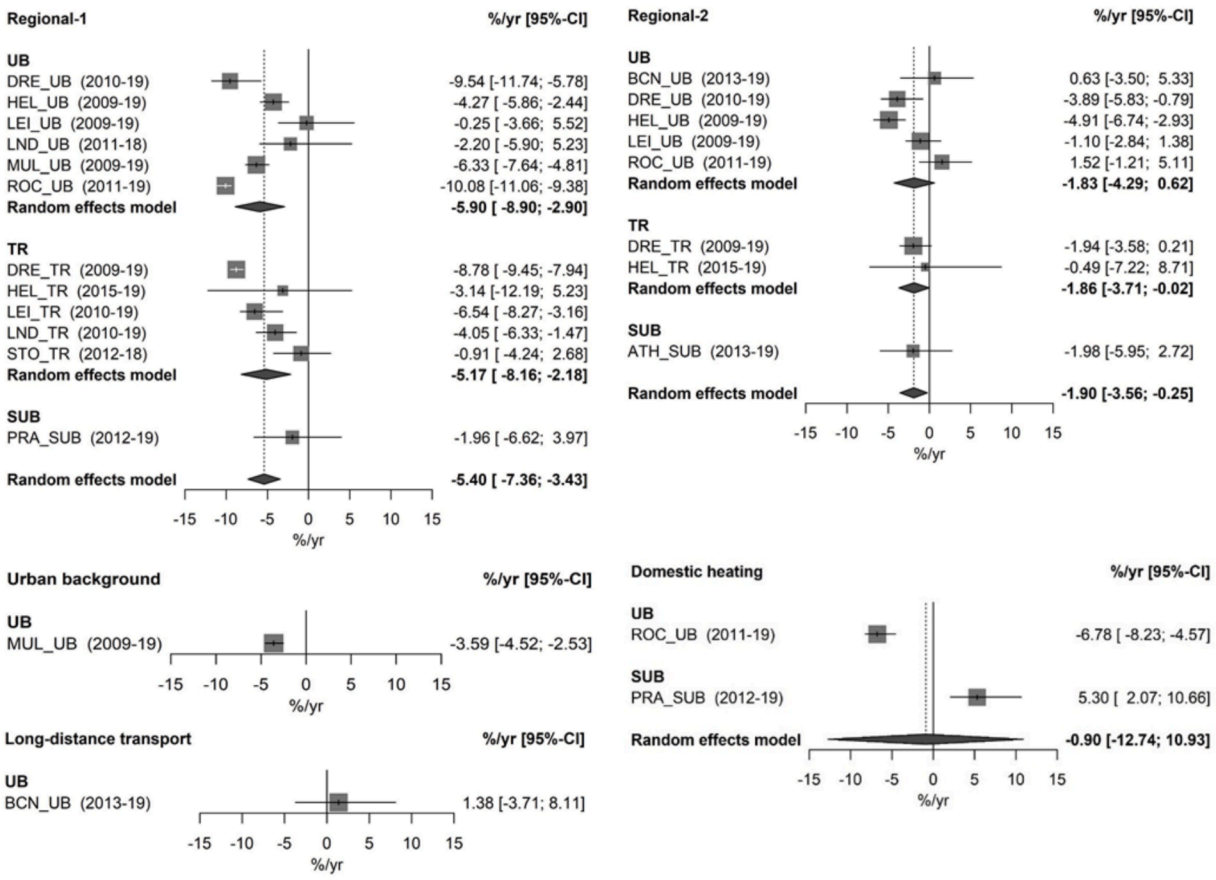

Fig. 7. Trend analysis and *meta*-analysis results for *Regional-1*, *Regional-2*, *Urban background*, *Domestic heating* and *Long-distance transport* sources. Trends are calculated using the Theil-Sen method. Mean effects for each site type (Urban background, UB; Traffic, TR; Suburban background, SUB; and Regional background, RB) are estimated using a random effects model. The *meta*-analysis results are presented for each pollutant across the different site types, as well as for global trends (dashed line).

implementation of European emission standards, especially after the introduction of diesel particle filters (DPFs) from the 2011 EURO 5/V standard for primary particles. The effect of DPFs is observed in the higher reduction of *Traffic-2* (primarily associated with diesel vehicle emissions) compared to *Traffic-1* (mainly gasoline vehicle emissions and nucleation of UFP from diesel). Furthermore, the reduction of sulphur (S) content in diesel might have contributed to reducing UFP from road traffic. However, ultra-low-S diesel (ULSD) was implemented in 2006 in Europe and the US, which was before the period covered by the datasets in this study. Other road traffic policy measures, such as Low Emission Zones (LEZ) in many cities and the Congestion Charge in some of them, also might have contributed to this reduction.

Traffic-Nucleation (and *Traffic-1* to a lesser extent) included the nucleation of particles generated during the dilution of diesel exhaust semi-volatile organic compounds (SVOCs), thus DPFs cannot retain them. This has prompted lighter decreasing trends for *Traffic-Nucleation* and *Traffic-1* (-2.97 % yr^{-1} and -2.78 % yr^{-1}) as compared with *Traffic-2* (-4.21 % yr^{-1}). Emission control technologies should be applied to DPFs to reduce the emissions of SVOCs. Furthermore, DPFs might be less efficient for particles smaller than 23 nm in diameter ($N_{<23}$). These results indicate that EURO standards should include emission controls for particle number concentration (PNC) for at least particles >10 nm and, if possible, for >1 nm, and not only for >23 nm, as the current standards have.

Trends in *Photonucleation* were more diverse among the sites. In some cases, this source increased probably due to a reduction in condensation sink, which facilitates photochemical NPF. In other cases, the reductions might be associated with the decrease of the emission of precursors of newly formed particles such as SO_2. The decrease in primary PM emissions and precursors of UFP also contributed to the reduction of urban and regional background sources.

The results of the study demonstrate the positive abatement of UFP in Europe, but more measures should be applied to reduce traffic emissions in the cities, especially an effort should be made to implement policies to reduce nucleated particles, both delayed primary diesel traffic particles and those from photochemical nucleation.

CRediT authorship contribution statement

Meritxell Garcia-Marlès: Writing – review & editing, Writing – original draft, Methodology, Formal analysis, Data curation, Conceptualization. **Rosa Lara:** Writing – review & editing, Writing – original draft, Methodology, Formal analysis, Data curation, Conceptualization. **Cristina Reche:** Writing – review & editing, Data curation. **Noemí Pérez:** Writing – review & editing, Data curation. **Aurelio Tobías:** Writing – review & editing, Methodology. **Marjan Savadkoohi:** Writing – review & editing, Data curation. **David Beddows:** Writing – review & editing, Data curation. **Imre Salma:** Writing – review & editing, Data curation. **Máté Vörösmarty:** Writing – review & editing, Data curation. **Tamás Weidinger:** Writing – review & editing, Data curation. **Christoph Hueglin:** Writing – review & editing, Data curation. **Nikos Mihalopoulos:** Writing – review & editing, Data curation. **Georgios Grivas:** Writing – review & editing, Data curation. **Panayiotis Kalkavouras:** Writing – review & editing, Data curation. **Jakub Ondracek:** Writing – review & editing, Data curation. **Nadezda Zikova:** Writing – review & editing, Data curation. **Jarkko V. Niemi:** Writing – review &

editing, Data curation. **Hanna E. Manninen:** Writing – review & editing, Data curation. **David C. Green:** Writing – review & editing, Data curation. **Anja H. Tremper:** Writing – review & editing, Data curation. **Michael Norman:** Writing – review & editing, Data curation. **Stergios Vratolis:** Writing – review & editing, Data curation. **Evangelia Diapouli:** Writing – review & editing, Data curation. **Konstantinos Eleftheriadis:** Writing – review & editing, Data curation. **Francisco J. Gómez-Moreno:** Writing – review & editing, Data curation. **Elisabeth Alonso-Blanco:** Writing – review & editing, Data curation. **Alfred Wiedensohler:** Writing – review & editing, Data curation. **Kay Weinhold:** Writing – review & editing, Data curation. **Maik Merkel:** Writing – review & editing, Data curation. **Susanne Bastian:** Writing – review & editing, Data curation. **Barbara Hoffmann:** Writing – review & editing, Data curation. **Hicran Altug:** Writing – review & editing, Data curation. **Jean-Eudes Petit:** Writing – review & editing, Data curation. **Prodip Acharja:** Writing – review & editing, Data curation. **Olivier Favez:** Writing – review & editing, Data curation. **Sebastiao Martins Dos Santos:** Writing – review & editing, Data curation. **Jean-Philippe Putaud:** Writing – review & editing, Data curation. **Adelaide Dinoi:** Writing – review & editing, Data curation. **Daniele Contini:** Writing – review & editing, Data curation. **Andrea Casans:** Writing – review & editing, Data curation. **Juan Andrés Casquero-Vera:** Writing – review & editing, Data curation. **Suzanne Crumeyrolle:** Writing – review & editing, Data curation. **Eric Bourrianne:** Writing – review & editing, Data curation. **Martine Van Poppel:** Writing – review & editing, Data curation. **Freja E. Dreesen:** Writing – review & editing, Data curation. **Sami Harni:** Writing – review & editing, Data curation. **Hilkka Timonen:** Writing – review & editing, Data curation. **Janne Lampilahti:** Writing – review & editing, Data curation. **Tuukka Petäjä:** Writing – review & editing, Data curation. **Marco Pandolfi:** Writing – review & editing, Data curation. **Philip K. Hopke:** Writing – review & editing, Data curation, Conceptualization. **Roy M. Harrison:** Writing – review & editing, Data curation, Conceptualization. **Andrés Alastuey:** Writing – review & editing, Writing – original draft, Data curation, Conceptualization. **Xavier Querol:** Writing – review & editing, Writing – original draft, Supervision, Methodology, Data curation, Conceptualization.

Declaration of competing interest

The authors declare that they have no known competing financial interests or personal relationships that could have appeared to influence the work reported in this paper.

Acknowledgements

This work is supported by the RI-URBANS project (Research Infrastructures Services Reinforcing Air Quality Monitoring Capacities in European Urban & Industrial Areas, European Union's Horizon 2020 research and innovation program, Green Deal, European Commission, contract 101036245), the "Agencia Estatal de Investigación" from the Spanish Ministry of Science and Innovation under the project CAIAC (PID2019-108990RB-I00), FEDER funds under the projects AIRPHONEMA (PID2022-142160OB-I00), and the Generalitat de Catalunya (AGAUR 2021 SGR 00447). It is also partly supported by the Hungarian Research, Development and Innovation Office (grant no. K132254). Marjan Savadkoohi thanks her FPI grant (PRE-2020-095498).

The authors acknowledge ACTRIS and National and City authorities for providing PNC-PNSD datasets.

Appendix A. Supplementary data

Supplementary data to this article can be found online at https://doi.org/10.1016/j.envint.2024.109149.

Data availability

Data will be made available on request.

References

ACTRIS, C. for A.I.-S.M., Preliminary, 2021. Preliminary ACTRIS recommendation for aerosol in-situ sampling, measurements, and analysis. https://www.actris.eu/sites/default/files/2021-06/Preliminary%20ACTRIS%20recommendations%20for%20aerosol%20in-situ%20measurements%20June%202021.pdf.

Al-Dabbous, A.N., Kumar, P., 2015. Source apportionment of airborne nanoparticles in a Middle Eastern city using positive matrix factorization. Environ. Science: Processes & Impacts 4 (17), 802. https://doi.org/10.1039/c5em00027k.

Amato, F., Hopke, P.K., 2012. Source apportionment of the ambient PM2.5 across St. Louis using constrained positive matrix factorization. Atmos. Environ. 46, 329–337. https://doi.org/10.1016/j.atmosenv.2011.09.062.

Amato, F., Alastuey, A., Karanasiou, A., Lucarelli, F., Nava, S., Calzolai, G., Severi, M., Becagli, S., Gianelle, V.L., Colombi, C., Alves, C., Custódio, D., Nunes, T., Cerqueira, M., Pio, C., Eleftheriadis, K., Diapouli, E., Reche, C., Minguillón, M.C., Manousakas, M.-I., Maggos, T., Vratolis, S., Harrison, R.M., Querol, X., 2016. AIRUSE-LIFE+: a harmonized PM speciation and source apportionment in five southern European cities. Atmos. Chem. Phys. 16, 3289–3309. https://doi.org/10.5194/acp-16-3289-2016.

Balduzzi, S., Rücker, G., Schwarzer, G., 2019. How to perform a meta-analysis with R: a practical tutorial. Evid. Based Ment. Health 22, 153–160. https://doi.org/10.1136/ebmental-2019-300117.

Beddows, D.C., Dall'Osto, M., Harrison, R.M., 2009. Cluster analysis of rural, urban, and curbside atmospheric particle size data. Environ. Sci. Technol. 43 (13), 4694–4700. https://doi.org/10.1021/es803121t.

Beddows, D.C.S., Harrison, R.M., Green, D.C., Fuller, G.W., 2015. Receptor modelling of both particle composition and size distribution from a background site in London. UK. Atmos. Chem. Phys. 15, 10107–10125. https://doi.org/10.5194/acp-15-10107-2015.

Beddows, D.C.S., Harrison, R.M., 2019. Receptor modelling of both particle composition and size distribution from a background site in London, UK – a two-step approach. Atmos. Chem. Phys. 19, 4863–4876. https://doi.org/10.5194/acp-19-4863-2019.

Belis C.A., Favez O., Mircea M., Diapouli E., Manousakas M.I., Vratolis S., Gilardoni S., Paglione M., Decesari S., Mocnik G., Mooibroek D., Salvador P., Takahama S., Vecchi R., Paatero P. 2019. European guide on air pollution source apportionment with receptor models - Revised version 2019. EUR 29816 EN. Joint Research Centre (European Commission). JRC117306. Publications Office of the European Union, Luxembourg, 2019. https://data.europa.eu/doi/10.2760/439106.

Bousiotis, D., Dall'Osto, M., Beddows, D.C.S., Pope, F.D., Harrison, R.M., 2019. Analysis of new particle formation (NPF) events at nearby rural, urban background and urban roadside sites. Atmos. Chem. Phys. 19, 5679–5694. https://doi.org/10.5194/acp-19-5679-2019.

Brean, J., Beddows, D.C.S., Shi, Z., Temime-Roussel, B., Marchand, N., Querol, X., Alastuey, A., Minguillón, M.C., Harrison, R.M., 2020. Molecular insights into new particle formation in Barcelona. Spain. Atmos. Chem. Phys. 20, 10029–10045. https://doi.org/10.5194/acp-20-10029-2020.

Brines, M., Dall'Osto, M., Beddows, D.C.S., Harrison, R.M., Querol, X., 2014. Simplifying aerosol size distribution modes simultaneously detected at four monitoring sites during SAPUSS. Atmos. Chem. Phys. 14, 2973–2986. https://doi.org/10.5194/acp-14-2973-2014.

Brines, M., Dall'Osto, M., Beddows, D.C.S., Harrison, R.M., Gómez-Moreno, F., Núñez, L., Artíñano, B., Costabile, F., Gobbi, G.P., Salimi, F., Morawska, L., Sioutas, C., Querol, X., 2015. Traffic and nucleation events as main sources of ultrafine particles in high-insolation developed world cities. Atmos. Chem. Phys. 15, 5929–5945. https://doi.org/10.5194/acp-15-5929-2015.

Carnerero, C., Pérez, N., Petäjä, T., Laurila, T.M., Ahonen, L.R., Kontkanen, J., Ahn, K.H., Alastuey, A., Querol, X., 2019. Relating high ozone, ultrafine particles, and new particle formation episodes using cluster analysis. Atmos. Environ. 4, 100051. https://doi.org/10.1016/j.aeaoa.2019.100051.

Carslaw, D.C., Ropkins, K., 2012. Openair - an R package for air quality data analysis. Environ. Model. Software 27 (28), 52–61. https://doi.org/10.1016/j.envsoft.2011.09.008.

Casquero-Vera, J.A., Lyamani, H., Titos, G., Minguillón, M.C., Dada, L., Alastuey, A., Querol, X., Petäjä, T., Olmo, F.J., Alados-Arboledas, L., 2021. Quantifying traffic, biomass burning and secondary source contributions to atmospheric particle number concentrations at urban and suburban sites. Sci. Total Environ. 768, 145282. https://doi.org/10.1016/j.scitotenv.2021.145282.

Cassee, F., Morawska, L., Peters, A., 2019. The White Paper on Ambient Ultrafine Particles: evidence for policy makers. 'Thinking outside the box' Team, 23 pp, https://efca.net/files/WHITE%20PAPER-UFP%20evidence%20for%20policy%20makers%20(25%20OCT).pdf.

CEN, 2020. CEN/TS 17434:2020. CEN Standard for Ambient air - Determination of the particle number size distribution of atmospheric aerosol using a Mobility Particle Size Spectrometer (MPSS). https://standards.iteh.ai/catalog/standards/cen/a841bc08-ed34-4fa8-94ca-8c5e07b99db9/cen-ts-17434-2020.

Cesari, D., De Benedetto, G.E., Bonasoni, P., Busetto, M., Dinoi, A., Merico, E., Chirizzi, D., Cristofanelli, P., Donateo, A., Grasso, F.M., Marinoni, A., Pennetta, A., Contini, D., 2018. Seasonal variability of PM2.5 and PM10 composition and sources in an urban background site in Southern Italy. Sci. Total Environ. 612, 202–213. https://doi.org/10.1016/j.scitotenv.2017.08.230.

Chan, T.W., Mozurkewich, M., 2007. Simplified representation of atmospheric aerosol size distributions using absolute principal component analysis. Atmos. Chem. Phys. 7, 875–886. https://doi.org/10.5194/acp-7-875-2007.
Charron, A., Harrison, R.M., 2003. Primary particle formation from vehicle emissions during exhaust dilution in the roadside atmosphere. Atmos. Environ. 37 (29), 4109–4119. https://doi.org/10.1016/S1352-2310(03)00510-7.
Chen, L., Qi, X., Nie, W., Wang, J., Xu, Z., Wang, T., Liu, Y., Shen, Y., Xu, Z., Kokkonen, T. V., Chi, X., Aalto, P.P., Paasonen, P., Kerminen, V.M., Petäjä, T., Kulmala, M., Ding, A., 2021. Cluster analysis of submicron particle number size distributions at the SORPES station in the Yangtze River Delta of East China. Journal of Geophysical Research: Atmosphere 126. https://doi.org/10.1029/2020JD034004.
Chen, Y., Tian, C., Feng, Y., Zhi, G., Li, J., Zhang, G., 2015. Measurements of emission factors of PM2.5, OC, EC, and BC for household stoves of coal combustion in China. Atmos. Environ. 109, 190–196. https://doi.org/10.1016/j.atmosenv.2015.03.023.
Chen, Y., Masiol, M., Squizzato, S., Chalupa, D.C., Zíková, N., Pokorná, P., Rich, D.Q., Hopke, P.K., 2022. Long-term trends of ultrafine and fine particle number concentrations in New York State: apportioning between emissions and dispersion. Environ. Pollut. 310, 119797. https://doi.org/10.1016/j.envpol.2022.119797.
Corsini, E., Marinovich, M., Vecchi, R., 2019. Ultrafine particles from residential biomass combustion: a review on experimental data and toxicological response. Int. J. Mol. Sci. 20 (20), 4992. https://doi.org/10.3390/ijms20204992.
Cusack, M., Pérez, N., Pey, J., Alastuey, A., Querol, X., 2013. Source apportionment of fine PM and sub-micron particle number concentrations at a regional background site in the western Mediterranean: a 2.5 year study. Atmos. Chem. Phys. 13, 10, 5173–5187. https://doi.org/10.5194/acp-13-5173-2013.
Dall'Osto, M., Harrison, R.M., Coe, H., Williams, P.I., Allan, J.D., 2009. Real time chemical characterization of local and regional nitrate aerosols. Atmos. Chem. Phys. 9, 3709–3720. https://doi.org/10.5194/acp-9-3709-2009.
Dall'Osto, M., Thorpe, A., Beddows, D.C.S., Harrison, R.M., Barlow, J.F., Dunbar, T., Williams, P.I., Coe, H., 2011. Remarkable dynamics of nanoparticles in the urban atmosphere. Atmos. Chem. Phys. 11, 6623–6637. https://doi.org/10.5194/acp-11-6623-2011.
Dall'Osto, M., Beddows, D.C.S., Pey, J., Rodriguez, S., Alastuey, A., Harrison, R.M., Querol, X., 2012. Urban aerosol size distributions over the Mediterranean city of Barcelona, NE Spain. Atmos. Chem. Phys. 12, 10693–10707. https://doi.org/10.5194/acp-12-10693-2012.
Dall'Osto, M., Beddows, D.C.S., Tunved, P., Harrison, R.M., Lupi, A., Vitale, V., Becagli, S., Traversi, R., Park, K.T., Yoon, Y.J., Massling, A., Skov, H., Lange, R., Strom, J., Krejci, R., 2019. Simultaneous measurements of aerosol size distributions at three sites in the European high Arctic. Atmos. Chem. Phys. 19, 7377–7395. https://doi.org/10.5194/acp-19-7377-2019.
Damayanti, S., Harrison, R.M., Pope, F., Beddows, D.C.S., 2023. Limited impact of diesel particle filters on road traffic emissions of ultrafine particles. Environ. Int. 174, 107888. https://doi.org/10.1016/j.envint.2023.107888.
De la Sota, C., Lumbreras, J., Pérez, N., Ealo, M., Kane, M., Youm, I., Viana, M., 2018. Indoor air pollution from biomass cookstoves in rural Senegal. Energy Sustain. Dev. 43, 224–234. https://doi.org/10.1016/j.esd.2018.02.002.
Dinoi, A., Gulli, D., Ammoscato, I., Calidonna, C.R., Contini, D., 2021. Impact of the coronavirus pandemic lockdown on atmospheric nanoparticle concentrations in two sites of Southern Italy. Atmos. 12, 352. https://doi.org/10.3390/atmos12030352.
EC, 2008. Directive 2008/50/EC of the European Parliament and of the Council of 21 May 2008 on ambient air quality and cleaner air for Europe. https://eur-lex.europa.eu/legal-content/EN/TXT/?uri=CELEX:32008L0050.
EC, 2023. Proposal for a Directive of the European Parliament and of the Council on ambient air quality and cleaner air for Europe (recast) - Mandate for negotiations with the European Parliament. https://data.consilium.europa.eu/doc/document/ST-15236-2023-NIT/en/pdf.
EEA, 2023. Air pollution in Europe: 2023 reporting status under the National Emission Reduction Commitments Directive. https://doi.org/10.2800/339055.
Ehn, M., Thornton, J., Kleist, E., Sipilä, M., Junninen, H., Pullinen, I., Springer, M., Rubach, F., Tillmann, R., Lee, B., Lopez-Hilfiker, F., Andres, S., Acir, I.H., Rissanen, M., Jokinen, T., Schobesberger, S., Kangasluoma, J., Kontkanen, J., Nieminen, T., Kurtén, T., Nielsen, L.B., Jørgensen, S., Kjaergaard, H.G., Canagaratna, M., Dal Maso, M., Berndt, T., Petäjä, T., Wahner, A., Kerminen, V.M., Kulmala, M., Worsnop, D.R., Wildt, J., Mentel, T.F., 2014. A large source of low-volatility secondary organic aerosol. Nature 506, 476–479. https://doi.org/10.1038/nature13032.
Eleftheriadis, K., Gini, M.I., Diapouli, E., Vratolis, S., Vasilatou, V., Fetfatzis, P., Manousakas, M.I., 2021. Aerosol microphysics and chemistry reveal the COVID19 lockdown impact on urban air quality. Sci. Rep. 11, 14477. https://doi.org/10.1038/s41598-021-93650-6.
Gangoiti, G., Millán, M.M., Salvador, R., Mantilla, E., 2001. Long-range transport and re-circulation of pollutants in the western Mediterranean during the project regional cycles of air pollution in the west-central mediterranean area. Atmos. Environ. 35 (36), 6267–6276. https://doi.org/10.1016/S1352-2310(01)00440-X.
Garcia-Marlès, M., Lara, R., Reche, C., Pérez, N., Tobías, A., Savadkoohi, M., Beddows, D., Salma, I., Vörösmarty, M., Weidinger, T., Hueglin, C., Mihalopoulos, N., Grivas, G., Kalkavouras, P., Ondráček, J., Zíková, N., Niemi, J.V., Manninen, H.E., Green, D.C., Tremper, A.H., Norman, M., Vratolis, S., Eleftheriadis, K., Gómez-Moreno, F.J., Alonso-Blanco, E., Wiedensohler, A., Weinhold, K., Merkel, M., Bastian, S., Hoffmann, B., Altug, H., Petit, J.E., Favez, O., Dos Santos, S.M., Putaud, J.P., Dinoi, A., Contini, D., Timonen, H., Lampilahti, J., Petäjä, T., Pandolfi, M., Hopke, P.K., Harrison, R.M., Alastuey, A., Querol, X., 2024. Inter-annual trends of ultrafine particles in urban Europe. Environ. Int. 185, 108510. https://doi.org/10.1016/j.envint.2024.108510.
Gu, J., Pitz, M., Schnelle-Kreis, J., Diemer, J., Reller, A., Zimmermann, R., Soentgen, J., Stoelzel, M., Wichmann, H.E., Peters, A., Cyrys, J., 2011. Source apportionment of ambient particles: comparison of positive matrix factorization analysis applied to particle size distribution and chemical composition data. Atmos. Environ. 45 (10), 1849–1857. https://doi.org/10.1016/j.atmosenv.2011.01.009.
Hamed, A., Joutsensaari, J., Mikkonen, S., Sogacheva, L., Dal Maso, M., Kulmala, M., Cavalli, F., Fuzzi, S., Facchini, M.C., Decesari, S., Mircea, M., Lehtinen, K.E.J., Laaksonen, A., 2007. Nucleation and growth of new particles in Po Valley. Italy. Atmos. Chem. Phys. 7, 355–376. https://doi.org/10.5194/acp-7-355-2007.
Harrison, R.M., Beddows, D.C.S., Dall'Osto, M., 2011. PMF analysis of wide-range particle size spectra collected on a major highway. Environ. Sci. Technol. 45, 5522–5528. https://doi.org/10.1021/es2006622.
Harrison, R.M., Jones, A.M., Beddows, D.C.S., Dall'Osto, M., Nikolova, I., 2016. Evaporation of traffic-generated nanoparticles during advection from source. Atmos. Environ. 125, 1–7. https://doi.org/10.1016/j.atmosenv.2015.10.077.
He, C., Li, J., Ma, Z., Tan, J., Zhao, L., 2015. High NO2/NOx emissions downstream of the catalytic diesel particulate filter: An influencing factor study. J. Environ. Sci. (China) 35, 55–61. https://doi.org/10.1016/j.jes.2015.02.009.
Hewson, E.W., 1955. Stack heights required to minimise ground concentrations. Trans. ASME 77 (7), 1163–1171. https://doi.org/10.1115/1.4014631.
Hopke, P.K., Feng, Y., Dai, Q., 2022. Source apportionment of particle number concentrations: a global review. Sci. Total Environ. 819, 153104. https://doi.org/10.1016/j.scitotenv.2022.153104.
Hopke, P.K., Chen, Y., Rich, D.Q., Mooibroek, D., Sofowote, U.M., 2023. The application of positive matrix factorization with diagnostics to BIG DATA. Chemom. Intell. Lab. Syst. 240, 104885. https://doi.org/10.1016/j.chemolab.2023.104885.
Hopke, P.K., Chen, Y., Chalupa, D.C., Rich, D.Q., 2024. Long term trends in source apportioned particle number concentrations in Rochester NY. Environ. Pollut. 347, 123708. https://doi.org/10.1016/j.envpol.2024.123708.
Ibald-Mulli, A., Wichmann, H.E., Kreyling, W., Peters, A., 2004. Epidemiological evidence on health effects of ultrafine particles. J. Aerosol Med. Pulm. Drug Deliv. 15 (2), 189–201. https://doi.org/10.1089/089426802320282310.
ISO, 2023. ISO 80004-1:2023. Nanotechnologies – Vocabulary — Part 1: Core vocabulary. https://www.iso.org/standard/79525.html.
Junkermann, W., Hacker, J.M., 2018. Ultrafine particles in the lower troposphere: major sources, invisible plumes, and meteorological transport processes. Am. Meteorol. Soc. 2587–2602. https://doi.org/10.1175/BAMS-D-18-0075.1.
Junkermann, W., Hagemann, R., Vogel, B., 2011. Nucleation in the Karlsruhe plume during the COPS/TRACKS-Lagrange experiment. Quart. J. Royal Meteorol. Soc. 137, 267–274. https://doi.org/10.1002/qj.753.
Junkermann, W., Vogel, B., Bangert, M., 2016. Ultrafine particles over Germany - an aerial survey. Tellus b: Chem. Phys. Meteorol. 68 (1), 29250. https://doi.org/10.3402/tellusb.v68.29250.
Kalkavouras, P., Bougiatioti, A., Grivas, G., Stavroulas, I., Kalivitis, N., Liakakou, E., Gerasopoulos, E., Pilinis, C., Mihalopoulos, N., 2020. On the regional aspects of new particle formation in the Eastern Mediterranean: a comparative study between a background and an urban site based on long term observations. Atmos. Res. 239, 104911. https://doi.org/10.1016/j.atmosres.2020.104911.
Kalkavouras, P., Grivas, G., Stavroulas, I., Petrinoli, K., Bougiatioti, A., Liakakou, E., Gerasopoulos, E., Mihalopoulos, N., 2024. Source apportionment of fine and ultrafine particle number concentrations in a major city of the Eastern Mediterranean. Sci. Total Environ. 915, 170042. https://doi.org/10.1016/j.scitotenv.2024.170042.
Kalogridis, A.C., Vratolis, S., Liakakou, E., Gerasopoulos, E., Mihalopoulos, N., Eleftheriadis, K., 2018. Assessment of wood burning versus fossil fuel contribution to wintertime black carbon and carbon monoxide concentrations in Athens. Greece. Atmos. Chem. Phys. 18, 10219–10236. https://doi.org/10.5194/acp-18-10219-2018.
Kasumba, J., Hopke, P.K., Chalupa, D.C., Utell, M.J., 2009. Comparison of sources of submicron particle number concentrations measured at two sites in Rochester. NY. Sci. Total Environ. 407, 5071–5084. https://doi.org/10.1016/j.scitotenv.2009.05.040.
Keuken, M.P., Moerman, M., Zandveld, P., Henzing, J.S., Hoek, G., 2015. Total and size-resolved particle number and black carbon concentrations in urban areas near Schiphol airport (the Netherlands). Atmos. Environ. 104, 132–142. https://doi.org/10.1016/j.atmosenv.2015.01.015.
Khan, M.F., Latif, M.T., Amil, N., Juneng, L., Mohamad, N., Nadzir, M.S., Hoque, H.M., 2015. Characterization and source apportionment of particle number concentration at a semi-urban tropical environment. Environ. Sci. Pollut. Res. Int. 22 (17), 13111–13126. https://doi.org/10.1007/s11356-015-4541-4.
Kleeman, M.J., Riddle, S.G., Robert, M.A., Jakober, C.A., Fine, P.M., Hays, M.D., Schauer, J.J., Hannigan, M.P., 2009. Source apportionment of fine (PM1.8) and ultrafine (PM0.1) airborne particulate matter during a severe winter pollution episode. Environ. Sci. Technol. 43, 2, 272–279. https://doi.org/10.1021/es800400m.
Kreyling, W.G., Hirn, S., Möller, W., Schleh, C., Wenk, A., Celik, G., Lipka, J., Schäffler, M., Haberl, N., Johnston, B.D., Sperling, R., Schmid, G., Simon, U., Parak, W.J., Semmler-Behnke, M., 2014. Air-blood barrier translocation of tracheally instilled gold nanoparticles inversely depends on particle size. ACS Nano 8 (1), 222–233. https://doi.org/10.1021/nn403256v.
Kulmala, M., Kerminen, V.M., 2008. On the formation and growth of atmospheric nanoparticles. Atmos. Res. 90 (2–4), 132–150. https://doi.org/10.1016/j.atmosres.2008.01.005.
Kulmala, M., Luoma, K., Virkkula, A., Petäjä, T., Paasonen, P., Kerminen, V.M., Nie, W., Qi, X., Shen, Y., Chi, X., Ding, A., 2016. On the mode-segregated aerosol particle

number concentration load: contributions of primary and secondary particles in Hyytiälä and Nanjing. Boreal Env. Res. 21, 319–331.
Kulmala, M., Kerminen, V.M., Petaja, T., Ding, A.J., Wang, L., 2017. Atmospheric gas-to-particle conversion: why NPF events are observed in megacities? Faraday Discuss. 200, 271–288. https://doi.org/10.1039/c6fd00257a.
Kumar, P., Morawska, L., Birmili, W., Paasonen, P., Hug, M., Kulmala, M., Harrison, R. M., Norfordj, L., Britter, R., 2014. Ultrafine particles in cities. Environ. Int. 66, 1–10. https://doi.org/10.1016/j.envint.2014.01.013.
Kuye, A., Kumar, P., 2023. A review of the physicochemical characteristics of ultrafine particle emissions from domestic solid fuel combustion during cooking and heating. Sci. Total Environ. 886, 163747. https://doi.org/10.1016/j.scitotenv.2023.163747.
Liu, X., Hadiatullah, H., Zhang, X., Trechera, P., Savadkoohi, M., Garcia-Marlès, M., Reche, C., Pérez, N., Beddows, D.C.S., Salma, I., Thén, W., Kalkavouras, P., Mihalopoulos, N., Hueglin, C., Green, D.C., Tremper, A.H., Chazeau, B., Gille, G., Marchand, N., Niemi, J.V., Manninen, H.E., Portin, H., Zíková, N., Ondracek, J., Norman, M., Gerwig, H., Bastian, S., Merkel, M., Weinhold, K., Casans, A., Casquero-Vera, J.A., Gómez-Moreno, F.J., Artíñano, B., Gini, M., Diapouli, E., Crumeyrolle, S., Riffault, V., Petit, J.E., Favez, O., Putaud, J.P., Dos Santos, S.M., Timonen, H., Aalto, P.P., Hussein, T., Lampilahti, J., Hopke, P.K., Wiedensohler, A., Harrison, R. M., Petäjä, T., Pandolfi, M., Alastuey, A., Querol, X., 2023. Ambient air particulate total lung deposited surface area (LDSA) levels in urban Europe. Sci. Total Environ. 898, 165466. https://doi.org/10.1016/j.scitotenv.2023.165466.
Liu, Z.R., Hu, B., Liu, Q., Sun, Y., Wang, Y.S., 2014. Source apportionment of urban fine particle number concentration during summertime in Beijing. Atmos. Environ. 96, 359–369. https://doi.org/10.1016/j.atmosenv.2014.06.055.
Lv, Y., Chen, X., Wei, S., Zhu, R., Wang, B., Chen, B., Kong, M., Zhang, J., 2020. Sources, concentrations, and transport models of ultrafine particles near highways: a Literature Review. Build. Environ. 186, 107325. https://doi.org/10.1016/j.buildenv.2020.107325.
Mamakos, A., Martini, G., 2011. Particle Number Emissions During Regeneration of DPF-equipped Light Duty Diesel Vehicles - a Literature Survey. EUR 24853 EN. Publications Office of the European Union, Luxembourg. JRC64870.
Masiol, M., Vu, T.V., Beddows, D.C.S., Harrison, R.M., 2016. Source apportionment of wide range particle size spectra and black carbon collected at the airport of Venice (Italy). Atmos. Environ. 139, 56–74. https://doi.org/10.1016/j.atmosenv.2016.05.018.
McMurry, P.H., Friedlander, S.K., 1979. New particle formation in the presence of an aerosol. Atmos. Environ. 13, 1635–1651. https://doi.org/10.1016/0004-6981(79)90322-6.
Mikkonen, S., Németh, Z., Varga, V., Weidinger, T., Leinonen, Yli-Juuti, T., Salma, I., 2020. Decennial time trends and diurnal patterns of particle number concentrations in a Central European city between 2008 and 2018. Atmos. Chem. Phys. 20, 12247–12263. https://doi.org/10.5194/acp-20-12247-2020.
Millán, M.M., Mantilla, E., Salvador, R., Carratalá, A., Sanz, M.J., Alonso, L., Gangoiti, G., Navazo, M., 2000. Ozone cycles in the western mediterranean basin: interpretation of monitoring data in complex coastal terrain. J. Appl. Meteorol. 39, 487–508. https://doi.org/10.1175/1520-0450(2000)039<0487:OCITWM>2.0.CO;2.
Nie, D., Qiu, Z., Wang, X., Liu, Z., 2022. Characterizing the source apportionment of black carbon and ultrafine particles near urban roads in Xi'an. China. Environ. Res. 215 (1), 114209. https://doi.org/10.1016/j.envres.2022.114209.
Norris, G., Duvall, R., Brown, S., Bai, S., 2014. EPA Positive Matrix Factorization (PMF) 5.0 Fundamentals and User Guide. U.S. Environmental Protection Agency, Washington, DC. EPA/600/R-14/108 (NTIS PB2015-105147).
Oberdörster, G., Oberdörster, E., Oberdörster, J., 2005. Nanotoxicology: an emerging discipline evolving from studies of ultrafine particles. Environ. Health Perspect. 113, 823–839. https://doi.org/10.1289/ehp.7339.
Ogulei, D., Hopke, P.K., Chalupa, D.C., Utell, M.J., 2007. Modeling source contributions to submicron particle number concentrations measured in rochester. New York. Aerosol Sci. Technol. 41, 179–201. https://doi.org/10.1080/02786820601116012.
Ohlwein, S., Kappeler, R., Joss, M.K., Künzli, N., Hoffmann, B., 2019. Health effects of ultrafine particles: a systematic literature review update of epidemiological evidence. Int. J. Public Health 64 (4), 547–559. https://doi.org/10.1007/s00038-019-01202-7.
Oliveira, C., Alves, c., Pio, C.A., 2009. Aerosol particle size distributions at a traffic exposed site and an urban background location in Oporto. Portugal. Quim. Nova 32 (4), 928–933. https://doi.org/10.1590/S0100-40422009000400019.
Paatero, P., 1999. The multilinear engine: a table-driven, least squares program for solving multilinear problems, including the n-way parallel factor analysis model. J. Comput. Graph. Stat. 8 (4), 854–888. https://doi.org/10.2307/1390831.
Paatero, P., Tapper, U., 1994. Positive matrix factorization: a non-negative factor model with optimal utilization of error estimates of data values. Environmetrics 5 (2), 111–126. https://doi.org/10.1002/env.3170050203.
Pancras, J.P., Landis, M.S., Norris, G.A., Vedantham, R., Dvonch, J.T., 2013. Source apportionment of ambient fine particulate matter in Dearborn, Michigan, using hourly resolved PM chemical composition data. Sci. Total Environ. 15 (448), 2–13. https://doi.org/10.1016/j.scitotenv.2012.11.083.
Patel, H., Talbot, N., Salmond, J., 2023. The impact of low emission zones on personal exposure to ultrafine particles in the commuter environment. Sci. Total Environ. 874, 162540. https://doi.org/10.1016/j.scitotenv.2023.162540.
Peters, A., Veronesi, B., Calderón-Garcidueñas, L., Gehr, P., Chen, L.C., Geiser, M., Reed, W., Rothen-Rutishauser, B., Schürch, S., Schulz, H., 2006. Translocation and potential neurological effects of fine and ultrafine particles a critical update. Part. Fibre. Toxicol. 3, 13. https://doi.org/10.1186/1743-8977-3-13.
Petit, J.E., Dupont, J.C., Favez, O., Gros, V., Zhang, Y., Sciare, J., Simon, L., Truong, F., Bonnaire, N., Amodeo, T., Vautard, R., Haeffelin, M., 2021. Response of atmospheric composition to COVID-19 lockdown measures during spring in the Paris region (France). Atmos. Chem. Phys. 21 (22), 17167–17183. https://doi.org/10.5194/acp-21-17167-2021.
Pey, J., Querol, X., Alastuey, A., Rodríguez, S., Putaud, J.P., Van Dingenen, R., 2009. Source Apportionment of urban fine and ultrafine particle number concentration in a Western Mediterranean city. Atmos. Environ. 43, 4407–4415. https://doi.org/10.1016/j.atmosenv.2009.05.024.
Polissar, A.V., Hopke, P.K., Paatero, P., 1998. Atmospheric aerosol over Alaska - 2. Elemental composition and sources. J. Geophys. Res. Atmos. 103, 19045–19057. https://doi.org/10.1029/98JD01212.
Preble, C.V., Harley, R.A., Kirchstetter, T.W., 2019. Control technology-driven changes to in-use heavy-duty diesel truck emissions of nitrogenous species and related environmental impacts. Environ. Sci. Technol. 53, 14568–14576. https://doi.org/10.1021/acs.est.9b04763.
Presto, A.A., Saha, P.K., Robinson, A.L., 2021. Past, present, and future of ultrafine particle exposures in North America. Atmos. Environ. 10, 100109. https://doi.org/10.1016/j.aeaoa.2021.100109.
Putaud, J.P., Pozzoli, L., Pisoni, E., Martins Dos Santos, S., Lagler, F., Lanzani, G., Dal Santo, U., Colette, A., 2021. Impacts of the COVID-19 lockdown on air pollution at regional and urban background sites in northern Italy. Atmos. Chem. Phys. 21, 7597–7609. https://doi.org/10.5194/acp-21-7597-2021.
Putaud, J.P., Pisoni, E., Mangold, A., Hueglin, C., Sciare, J., Pikridas, M., Savvides, C., Ondracek, J., Mbengue, S., Wiedensohler, A., Weinhold, K., Merkel, M., Poulain, L., van Pinxteren, D., Herrmann, H., Massling, A., Nordstroem, C., Alastuey, A., Reche, C., Pérez, N., Castillo, S., Sorribas, M., Adame, J.A., Petaja, T., Lehtipalo, K., Niemi, J., Riffault, V., de Brito, J.F., Colette, A., Favez, O., Petit, J.E., Gros, V., Gini, M.I., Vratolis, S., Eleftheriadis, K., Diapouli, E., Denier van der Gon, H., Yttri, K. E., Aas, W., 2023. Impact of 2020 COVID-19 lockdowns on particulate air pollution across Europe. Atmos. Chem. Phys. 23, 10145–10161. https://doi.org/10.5194/acp-23-10145-2023.
Qian, S., Sakurai, H., McMurry, P.H., 2007. Characteristics of regional nucleation events in urban East St. Louis. Atmos. Environ. 41 (19), 4119–4127. https://doi.org/10.1016/j.atmosenv.2007.01.011.
R Core Team, 2023. R: A Language and Environment for Statistical Computing. R Foundation for Statistical Computing, Vienna, Austria. https://www.R-project.org/.
Reche, C., Querol, X., Alastuey, A., Viana, M., Pey, J., Moreno, T., Rodríguez, S., González, Y., Fernández-Camacho, R., de la Rosa, J., Dall'Osto, M., Prévôt, A.S.H., Hueglin, C., Harrison, R.M., Quincey, P., 2011. New considerations for PM, black carbon and particle number concentration for air quality monitoring across different European cities. Atmos. Chem. Phys. 11, 6207–6227. https://doi.org/10.5194/acp-11-6207-2011.
RI-URBANS, 2022. Guidelines, datasets of non-regulated pollutants incl. metadata, methods. Deliverable D1 (D1.1). 71 pp. https://riurbans.eu/wp-content/uploads/2022/10/RI-URBANS_D1_D1_1.pdf.
Rivas, I., Beddows, D.C.S., Amato, F., Green, D.C., Järvi, L., Hueglin, C., Reche, C., Timonen, H., Fuller, G.W., Niemi, J.V., Pérez, N., Aurela, M., Hopke, P.K., Alastuey, A., Kulmala, M., Harrison, R.M., Querol, X., Kelly, F.J., 2019. Source apportionment of particle number size distribution in urban background and traffic stations in four European cities. Environ. Int. 135, 105345. https://doi.org/10.1016/j.envint.2019.105345.
Rivas, I., Vicens, L., Basagaña, X., Tobías, X., Katsouyanni, K., Walton, H., Hüglin, C., Alastuey, A., Kulmala, M., Harrison, R.M., Pekkanen, J., Querol, X., Sunyer, J., Kelly, F.J., 2021. Associations between sources of particle number and mortality in four European cities. Environ. Int. 155, 106662. https://doi.org/10.1016/j.envint.2021.106662.
Rodríguez, S., Cuevas, E., 2007. The contributions of "minimum primary emissions" and "new particle formation enhancements" to the particle number concentration in urban air. Aerosol Sci. 38, 1207–1219. https://doi.org/10.1016/j.jaerosci.2007.09.001.
Rönkkö, T., Kuuluvainen, H., Karjalainen, P., Keskinen, J., Hillamo, R., Niemi, J.V., Pirjola, L., Timonen, H.J., Saarikoski, S., Saukko, E., Järvinen, A., Silvennoinen, H., Rostedt, A., Olin, M., Yli-Ojanperä, J., Nousiainen, P., Kousa, A., Dal Maso, M., 2017. Traffic is a major source of atmospheric nanocluster aerosol. Proc. Natl. Acad. Sci. USA 114, 7549–7554. https://doi.org/10.1073/pnas.1700830114.
Rönkkö, T., Timonen, H., 2019. Overview of sources and characteristics of nanoparticles in Urban Traffic-Influenced Areas. J. Alzheimers Dis. 72 (1), 15–28. https://doi.org/10.3233/JAD-190170.
Saarikoski, S., Järvinen, A., Markkula, L., Aurela, M., Kuittinen, N., Hoivala, J., Barreira, L.M.F., Aakko-Saksa, P., Lepistö, T., Marjanen, P., Timonen, H., Hakkarainen, H., Jalava, P., Rönkkö, T., 2024. Towards zero pollution vehicles by advanced fuels and exhaust aftertreatment technologies. Environ. Pollut. 347, 123665. https://doi.org/10.1016/j.envpol.2024.123665.
Saiz-Lopez, A., Borge, R., Notario, A., Adame, J.A., de la Paz, D., Querol, X., Artíñano, B., Gómez-Moreno, F.J., Cuevas, C.A., 2017. Unexpected increase in the oxidation capacity of the urban atmosphere of Madrid. Spain. Sci. Rep. 7, 45956. https://doi.org/10.1038/srep45956.
Salma, I., Füri, P., Németh, Z., Balásházy, I., Hofmann, W., Farkas, Á., 2015. Lung burden and deposition distribution of inhaled atmospheric urban ultrafine particles as the first step in their health risk assessment. Atmos. Environ. 104, 39–49. https://doi.org/10.1016/j.atmosenv.2014.12.060.
Salma, I., Vörösmarty, M., Gyöngyösi, A.Z., Thén, W., Weidinger, T., 2020. What can we learn about urban air quality with regard to the first outbreak of the COVID-19 pandemic? A case study from central Europe. Atmos. Chem. Phys. 20, 15725–15742. https://doi.org/10.5194/acp-20-15725-2020.
Salma, I., Thén, W., Aalto, P., Kerminen, V.-M., Kern, A., Barcza, Z., Petäjä, T., Kulmala, M., 2021. Influence of vegetation on occurrence and time distributions of

regional new aerosol particle formation and growth. Atmos. Chem. Phys. 21, 2861–2880. https://doi.org/10.5194/acp-21-2861-2021.
Schwarz, M., Schneider, A., Cyrys, J., Bastian, S., Breitner, S., Peters, A., 2023. Impact of ambient ultrafine particles on cause-specific mortality in three german cities. Am. J. Respir. Crit. Care Med. 207 (10), 1334–1344. https://doi.org/10.1164/rccm.202209-1837OC.
Seinfeld, J.H., Pandis, S., 2016. Atmospheric Chemistry and Physics: From Air Pollution to Climate Change, 3rd Edition. Wiley. ISBN 10: 1118947401.
Sen, P.K., 1968. Estimates of the regression coefficient based on Kendall's Tau. J. Am. Stat. Assoc. 63, 1379–1389.
Sicard, P., Agathokleous, E., De Marco, A., Paoletti, E., Calatayud, V., 2021. Urban population exposure to air pollution in Europe over the last decades. Environ. Sci. Eur. 33, 28. https://doi.org/10.1186/s12302-020-00450-2.
Simon, M.C., Naumova, E.N., Levy, J.I., Brugge, D., Durant, J.L., 2020. Ultrafine particle number concentration model for estimating retrospective and prospective long-term ambient exposures in Urban Neighborhoods. Environ. Sci. Technol. 54 (3), 1677–1686. https://doi.org/10.1021/acs.est.9b03369.
Sowlat, M.H., Hasheminassab, S., Sioutas, C., 2016. Source apportionment of ambient particle number concentrations in central Los Angeles using positive matrix factorization (PMF). Atmos. Chem. Phys. 16, 4849–4866. https://doi.org/10.5194/acp-16-4849-2016.
Spracklen, D.V., Carslaw, K.S., Merikanto, J., Mann, G.W., Reddington, C.L., Pickering, S., Ogren, J.A., Andrews, E., Baltensperger, U., Weingartner, E., Boy, M., Kulmala, M., Laakso, L., Lihavainen, H., Kivekäs, N., Komppula, M., Mihalopoulos, N., Kouvarakis, G., Jennings, S.G., O'Dowd, C., Birmili, W., Wiedensohler, A., Weller, R., Gras, J., Laj, P., Sellegri, K., Bonn, B., Krejci, R., Laaksonen, A., Hamed, A., Minikin, A., Harrison, R.M., Talbot, R., Sun, J., 2010. Explaining global surface aerosol number concentrations in terms of primary emissions and particle formation. Atmos. Chem. Phys. 10, 4775–4793. https://doi.org/10.5194/acp-10-4775-2010.
Squizzato, S., Masiol, M., Emami, F., Chalupa, D.C., Utell, M.J., Rich, D.Q., Hopke, P.K., 2019. Long-term changes of source apportioned particle number concentrations in a metropolitan area of the north-eastern United States. Atmos. 10 (1), 27. https://doi.org/10.3390/atmos10010027.
Stacey, B., Harrison, R.M., Pope, F., 2020. Evaluation of ultrafine particle concentrations and size distributions at London Heathrow Airport. Atmos. Environ. 222, 117148. https://doi.org/10.1016/j.atmosenv.2019.117148.
Taghvaee, S., Sowlat, M.H., Mousavi, A., Hassanvand, M.S., Yunesian, M., Naddafi, K., Sioutas, C., 2018. Source apportionment of ambient PM2.5 in two locations in central Tehran using the Positive Matrix Factorization (PMF) model. Sci. Total Environ. 628–629, 672–686. https://doi.org/10.1016/j.scitotenv.2018.02.096.
Theil H., 1992. A rank-invariant method of linear and polynomial regression analysis. In: Raj, B., Koerts, J. (Eds.), Henri Theil's Contributions to Economics and Econometrics, Advanced Studies in Theoretical and Applied Econometrics, vol. 23. Springer, Dordrecht. https://doi.org/10.1007/978-94-011-2546-8_20.
Tiwari, M., Sahu, S.K., Bhangare, R.C., Yousaf, A., Pandit, G.G., 2014. Particle size distributions of ultrafine combustion aerosols generated from household fuels. Atmos. Pollut. Res. 5 (1), 145–150. https://doi.org/10.5094/APR.2014.018.
Tobías, A., Rivas, I., Reche, C., Alastuey, A., Rodríguez, S., Fernández-Camacho, R., Sánchez de la Campa, A.M., de la Rosa, J., Sunyer, J., Querol, X., 2018. Short-term effects of ultrafine particles on daily mortality by primary vehicle exhaust versus secondary origin in three Spanish cities. Environ. Int. 111, 144–151. https://doi.org/10.1016/j.envint.2017.11.015.
Trechera, P., Garcia-Marlès, M., Liu, X.S., Reche, C., Perez, N., Savadkoohi, M., Beddows, D., Salma, I., Vörösmarty, M., Casans, A., Casquero-Vera, J.A., Hueglin, C., Marchand, N., Chazeau, B., Gille, G., Kalkavouras, P., Mihalopoulos, N., Ondracek, J., Zíková, N., Niemi, J.V., Manninen, H.E., Green, D.C., Tremper, A.H., Norman, M., Vratolis, S., Eleftheriadis, K., Gomez-Moreno, F.J., Alonso-Blanco, E., Gerwig, H., Wiedensohler, A., Weinhold, K., Merkel, M., Bastian, S., Petit, J.E., Favez, O., Crumeyrolle, S., Ferlay, N., Dos Santos, S.M., Putaud, J.P., Timonen, H., Lampilahti, J., Asbach, C., Wolf, C., Kaminski, H., Altug, H., Hoffmann, B., Rich, D. Q., Pandolfi, M., Harrison, R.M., Hopke, P.K., Petaja, T., Alastuey, A., Querol, X., 2023. Phenomenology of ultrafine particle concentrations and size distribution across urban Europe. Environ. Int. 172, 107744. https://doi.org/10.1016/j.envint.2023.107744.
US EPA, 2019. Integrated Science Assessment (ISA) for Particulate Matter (Final Report, Dec 2019). U.S. Environmental Protection Agency, Washington, DC, EPA/600/R-19/188. https://www.federalregister.gov/documents/2020/01/27/2020-01223/integrated-science-assessment-for-particulate-matter.
Vörösmarty, M., Hopke, P.K., Salma, I., 2024. Attribution of aerosol particle number size distributions to main sources using an 11-year urban dataset. Atmos. Chem. Phys. 24, 5695–5712. https://doi.org/10.5194/acp-24-5695-2024.
Wang, D., Li, Q., Shen, G., Deng, J., Zhou, W., Hao, J., Jiang, J., 2020. Significant ultrafine particle emissions from residential solid fuel combustion. Sci. Total Environ. 715, 136992. https://doi.org/10.1016/j.scitotenv.2020.136992.
Wegner, T., Hussein, T., Hämeri, K., Vesala, T., Kulmala, M., Weber, S., 2012. Properties of aerosol signature size distributions in the urban environment as derived by cluster analysis. Atmos. Environ. 61, 350–360. https://doi.org/10.1016/j.atmosenv.2012.07.048.
Wehner, B., Wiedensohler, A., 2003. Long term measurements of submicrometer urban aerosols: statistical analysis for correlations with meteorological conditions and trace gases. Atmos. Chem. Phys. 3, 867–879. https://doi.org/10.5194/acp-3-867-2003.
Wei, W., Zhang, W., Hu, D., Ou, L., Tong, Y., Shen, G., Shen, H., Wang, X., 2012. Emissions of carbon monoxide and carbon dioxide from uncompressed and pelletized biomass fuel burning in typical household stoves in China. Atmos. Environ. 56, 136–142. https://doi.org/10.1016/j.atmosenv.2012.03.060.
Weichenthal, S., Dufresne, A., Infante-Rivard, C., Joseph, L., 2008. Determinants of ultrafine particle exposures in transportation environments: findings of an 8-month survey conducted in Montréeal. Canada. J. Expo. Sci. Environ. Epidemiol. 18, 551–563. https://doi.org/10.1038/sj.jes.7500644.
Westerdahl, D., Fruin, S.A., Fine, P.L., Sioutas, C., 2008. The Los Angeles International Airport as a source of ultrafine particles and other pollutants to nearby communities. Atmos. Environ. 42 (13), 3143–3155. https://doi.org/10.1016/j.atmosenv.2007.09.006.
WHO, 2021a. Ambient (outdoor) air pollution. World Health Organization. https://www.who.int/news-room/fact-sheets/detail/ambient-(outdoor)-air-quality-and-health.
WHO, 2021b. WHO global air quality guidelines: particulate matter (PM2.5 and PM10), ozone, nitrogen dioxide, sulfur dioxide and carbon monoxide. World Health Organization. 273 pp, https://apps.who.int/iris/handle/10665/345329.
Wichmann, H.E., Spix, C., Tuch, T., Wölke, G., Peters, A., Heinrich, J., Kreyling, W.G., Heyder, J., 2000. Daily mortality and fine and ultrafine particles in Erfurt, Germany part I: role of particle number and particle mass. Rep. Health Effects Inst. 98, 5–98 (PMID: 11918089).
Wiedensohler, A., Wiesner, A., Weinhold, K., Birmili, W., Hermann, M., Merkel, M., Müller, T., Pfeifer, S., Schmidt, A., Tuch, T., Velarde, F., Quincey, P., Seeger, S., Nowak, A., 2018. Mobility particle size spectrometers: calibration procedures and measurement uncertainties. Aerosol Sci. Technol. 52, 146–164. https://doi.org/10.1080/02786826.2017.1387229.
Xu, W., Zhong, H., Lin, C., Huang, R.J., Ovadnevaite, J., Ceburnis, D., O'Dowd, C., 2024. Identification of sub-micrometer ambient sea salt number size distribution by positive matrix factorization. ACS EST Air. https://doi.org/10.1021/acsestair.3c00092.
Zhang, H., Zhu, T., Wang, S., Hao, J., Mestl, H.E.S., Alnes, L.W.H., Aunan, K., Dong, Z., Ma, L., Hu, Y., Zhang, M., Mellouki, A.W., Chai, F., Wang, S., 2014. Indoor emissions of carbonaceous aerosol and other air pollutants from household fuel burning in Southwest China. Aerosol Air Qual. Res. 14, 1779–1788. https://doi.org/10.4209/aaqr.2013.10.0305.
Zhou, L., Hopke, P.K., Stanier, C.O., Pandis, S.N., Ondov, J.M., Pancras, J.P., 2005. Investigation of the relationship between chemical composition and size distribution of airborne particles by partial least squares and positive matrix factorization. J. Geophys. Res. 110, D07S18. https://doi.org/10.1029/2004JD005050.
Zhu, Y., Hinds, W.C., Kim, S., Shen, S., Sioutas, C., 2002. Study of ultrafine particles near a major highway with heavy-duty diesel traffic. Atmos. Environ. 36, 4323–4335. https://doi.org/10.1016/S1352-2310(02)00354-0.
Zíková, N., Wang, Y., Yang, F., Li, X., Tian, M., Hopke, P.K., 2016. On the source contribution to Beijing PM2.5 concentrations. Atmos. Environ. 134, 84–95. https://doi.org/10.1016/j.atmosenv.2016.03.047.